Rates and mechanisms of sponge bioerosion

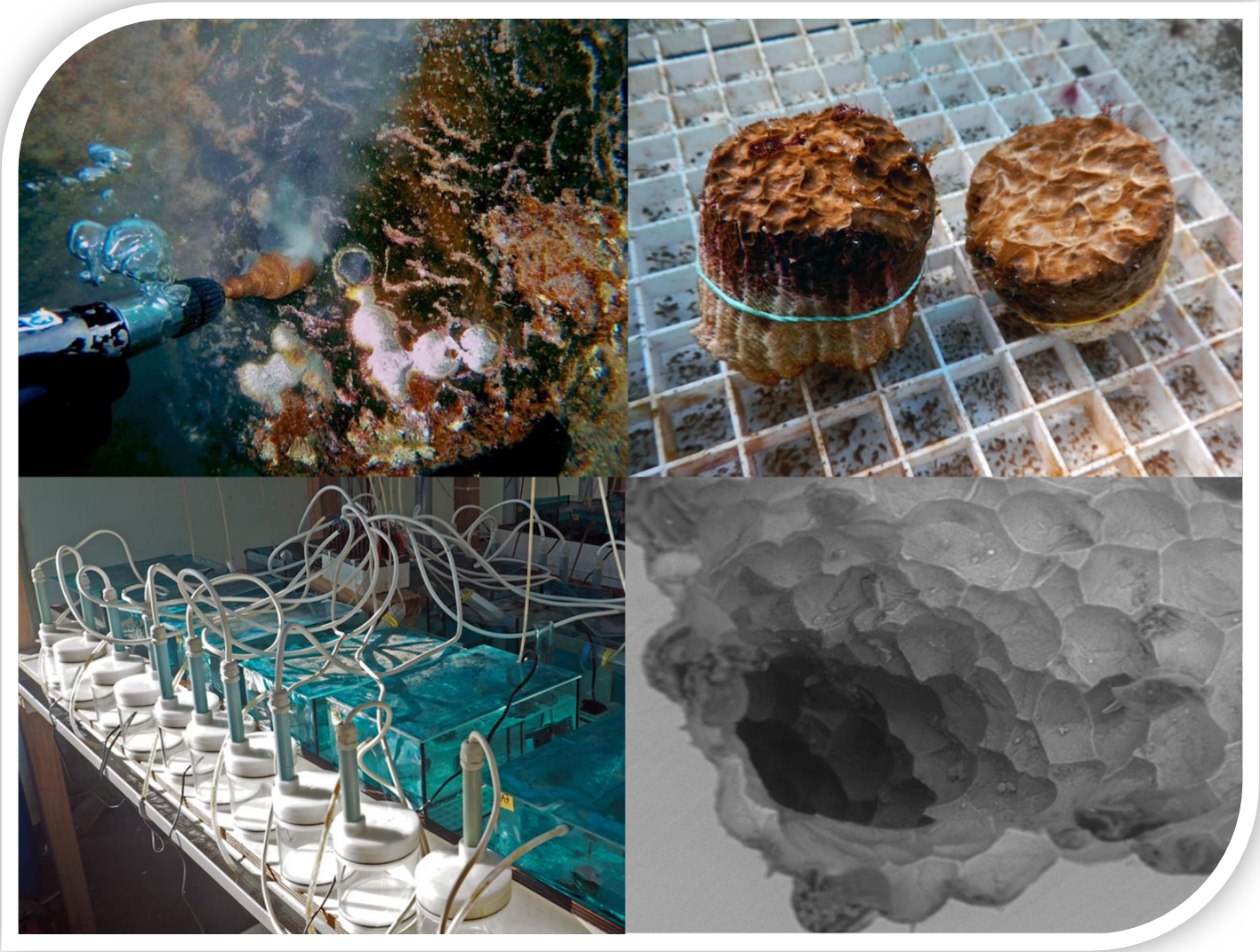

Master thesis research

Paul Peters
3831418
3-6-16

NIOZ

Universiteit Utrecht
Faculty of Geosciences

CNSI
CARIBBEAN NETHERLANDS SCIENCE INSTITUTE

Contents

Abstract

Coral reefs are complex marine ecosystems providing valuable economic and environmental services. These ecosystems are under serious threat worldwide due to global warming and ocean acidification. Particularly calcium carbonate producing marine organisms, such as corals, will suffer from the projected decrease in pH. Because the compounded effects of ocean acidification and warming significantly reduce reef-building potential, shifts in erosional processes could have substantial consequences for the carbonate budgets of coral reefs. Bioerosion by boring sponges, especially from the genus *Cliona*, has been shown to increase under acidification scenarios, but the mechanisms involved are poorly understood. Here, we decouple the covariance of $[H^+]$ and $[CO_3^{2-}]$ to reveal the individual effects of these parameters on the bioerosion rates of *C. caribbaea* during incubations. Varying these carbonate system parameters independently from each other revealed that high $[H^+]$ alone does not induce enhanced bioerosion. Instead, Ω constitutes a crucial threshold for bioeroding sponges; values above $\Omega \sim 4$ result in the sponge being unable to reduce Ω enough for dissolution to occur. Thus, Ω is the defining factor that governs whether and at which rate bioerosion occurs. Inspired by osteoclast bone resorption, the enzyme carbonic anhydrase II plays a central role in our hypothetical model for sponge bioerosion, which creates a framework for future study directions. By reducing the metabolic cost of both carbonate dissolution and the maintenance of ion gradients, the changes in chemistry due to ocean acidification enhance the bioerosion potential of clionaid sponges. Our findings confirm the present hypothesis that enhanced bioerosion rates are related to increased metabolic efficiency. The process of flushing is a potentially limiting factor for bioerosion rates and requires detailed, in-situ observations to reveal its underlying mechanisms. With enhanced bioerosion in future oceans alongside a decreased reef building potential of corals and calcifying algae, it seems inevitable that carbonate budgets will become increasingly negative.

1. Introduction

1.1 *Coral reefs are under threat*

Coral reefs are complex marine ecosystems providing valuable economic and environmental services. Their importance cannot be underestimated as they are essential for many local economies through tourism and fisheries and also provide coastal protection by buffering wave action and preventing erosion (Moberg & Folke, 1999). Given their contribution to human welfare, current trends in their decline are all the more alarming. Coral reefs are under serious threat worldwide, primarily due to over-harvesting (Jackson et al., 2001; Pandolfi et al., 2003), pollution (McCulloch et al., 2003; Williams et al., 2002), disease (Bourne et al., 2008; Burge et al., 2014) and climate change (Bellwood et al., 2004; Hoegh-Guldberg et al., 2007; Hughes et al., 2003). The latter poses the greatest threat because coral reefs already live near their physiological thresholds for temperature and seawater chemistry (Pandolfi et al., 2011).

1.2 *Climate change, ocean acidification and impacts on marine life*

Climate change is primarily driven by the burning of fossil fuels, which increased atmospheric CO_2 concentrations to 400 ppm (CO_2 Earth website, March 2016). This increase can be put into perspective considering that concentrations were around 280 ppm at the start of the industrial revolution in 1750. The rate of increase is unprecedented in geological history (Lüthi et al., 2008; Petit et al., 1999) and raises the question whether marine life will be able to adapt to the changes associated with this fast increase in CO_2 (Hoegh-Guldberg et al., 2007) The increase has been partially dampened because the ocean acts as a sink for anthropogenic CO_2 (Sabine et al., 2004). Accordingly, approximately 25% of the total CO_2 emitted by human activities since the industrial revolution has already been absorbed by the world's oceans (Canadell et al., 2007).

The absorption of additional CO_2 in seawater is termed ocean acidification (OA). When the partial pressure of CO_2 (pCO_2) in the atmosphere is higher than that of the underlying water column, CO_2 diffuses into the ocean (Fig. 1, Eq. 1) where most of the CO_2 reacts with water molecules to form carbonic acid (Eq. 2). This unstable compound quickly dissociates into a free hydrogen ion and a bicarbonate ion (Eq. 3). The protons released by reaction (3) lead to the decrease in oceanic pH that typifies ocean acidification (Raven et al., 2005).

$$CO_2(g) \rightleftharpoons CO_2(aq) \quad (1)$$

$$CO_2(aq) + H_2O(l) \rightleftharpoons H_2CO_3(aq) \quad (2)$$

$$H_2CO_3(aq) \rightleftharpoons H^+(aq) + HCO_3^-(aq) \quad (3)$$

$$HCO_3^-(aq) \rightleftharpoons H^+(aq) + CO_3^{2-}(aq) \quad (4)$$

$$\Omega = \frac{[Ca^{2+}][CO_3^{2-}]}{K_{sp}} \quad (5)$$

Fig. 1. The dissolution of CO_2 in seawater results in several reactions (Eq. 1-4), whereby the net effect is to increase the concentrations of H_2CO_3, HCO_3^- and H^+, and decrease the concentration of CO_3^{2-}, thereby lowering oceanic pH. Eq. 5 describes the saturation state of $CaCO_3$ (Ω); the product of $[Ca^{2+}]$ and $[CO_3^{2-}]$ divided by a solubility constant (K_{sp}) specific for the form of carbonate (e.g. aragonite in corals).

The anthropogenic acidification of the oceans is occurring at a rate unprecedented over at least the past 300 million years (Honisch et al., 2012) and has already dropped oceanic pH values by 0.1 pH unit since pre-industrial times. Since pH is measured on a logarithmic scale, this seemingly marginal decrease in pH represents a H^+ increase of almost 30% (Sabine et al., 2004) and thus a major change in one of the most basic environmental norms of marine life (Veron, 2011). With an ongoing decline of 0.3-0.4 pH units projected to occur by the end of the century (IPCC, 2007), both the rate and the scale of change in the oceans is significant for marine life.

Particularly calcium carbonate producing marine organisms will suffer from the projected decrease in pH; the protons formed during OA readily react with carbonate ions to form bicarbonate, in turn decreasing CO_3^{2-} concentration (Veron, 2011) (Eq. 4). The ability of these creatures to calcify largely depends on the saturation state of $CaCO_3$ (termed Ω), which consists of the product of $[Ca^{2+}]$ and $[CO_3^{2-}]$ divided by a solubility constant (K_{sp}: Eq. 5) specific for the form of carbonate. Thus when $[CO_3^{2-}]$ decreases due to OA, Ω decreases accordingly, likely hampering production of calcium carbonate and increasing dissolution rates of calcite and aragonite. Due to a higher K_{sp}, aragonite dissolves faster than calcite. This makes aragonite precipitating organisms such as corals especially vulnerable to OA and bioeroding organisms.

Indeed, many experimental studies have shown up to 40% reduced calcification rates in corals and foraminifers under altered pH or pCO_2 levels simulating projected future conditions (Anthony et al., 2008; Anthony et al., 2011; Hoegh-Guldberg et al., 2007; Kleypas & Langdon, 2006; Langdon & Atkinson, 2005; IPCC, 2007). Overall, the effect of OA on coral health, calcification, survival and reproduction has been shown to overwhelmingly negative (Anthony et al., 2011; Dufault et al., 2012; Marubini et al., 2008; McCulloch et al., 2012; Nakamura et al., 2011). Field studies have confirmed that net calcification on coral reefs approaches zero or even becomes negative at Ω values of 3.25, which would occur if atmospheric CO_2 concentrations ($[CO_2]_{atm}$) were to approach 480 ppm by the end of the century, dropping $[CO_3^{2-}]$ below 200 µmol kg^{-1} (Kleypas et al., 1999; Kleypas & Langdon, 2006). Simulation work by Hoegh-Guldberg et al. (2007) illustrates the potential marked decrease in saturation state in areas where warm water coral reefs are abundant (Fig. 2). With Ω values too low for net calcification to occur (Ω < 3.25), coral reefs would seize to grow (Veron et al., 2009).

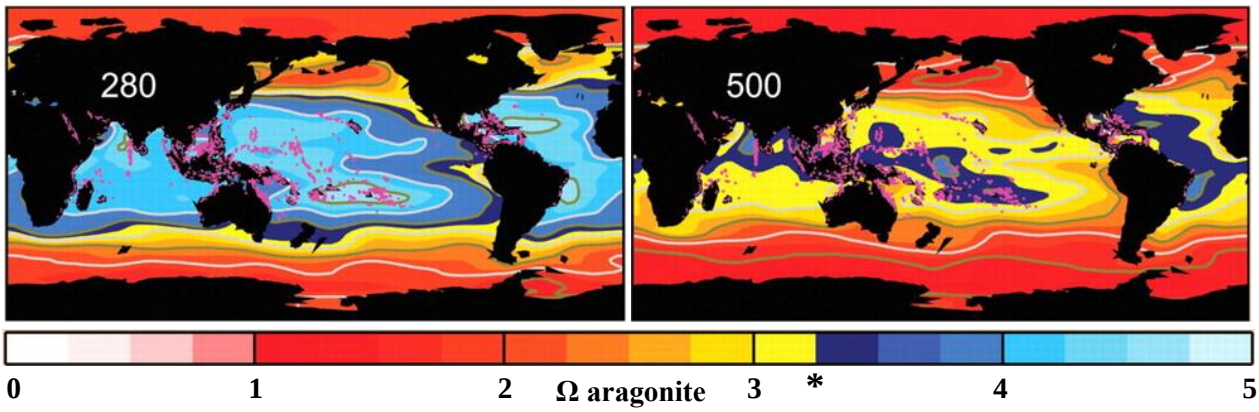

Fig. 2. The carbonate saturation state of aragonite is predicted to change upon increasing anthropogenic CO_2 concentrations. Nearly all shallow-water coral reefs (pink dots) had Ω values > 3.25 at the start of the industrial revolution (left pane, 280 ppm$[CO_2]_{atm}$). The number of reefs still above this vital Ω value (marked by an asterisk, *) is greatly diminished in future climate simulations (right pane, 500 ppm $[CO_2]_{atm}$). Present day conditions (not shown) reflect intermediate values between these two scenarios. Figure adapted from Hoegh-Guldberg et al. (2007).

1.3 The carbonate budget

The production and accumulation of reef framework is controlled by a dynamic balance between bioconstructional and (bio-)erosional processes. The relative rates of ecologically, physically and chemically driven processes all influence this balance, and ultimately, the carbonate budget of coral reefs (Montaggioni & Braithwaite, 2009; Perry et al., 2008). Corals usually form the primary (and dominant) framework producers on a reef, adding significant amounts of carbonate per unit area (Vecsei, 2004). Calcareous encrusters, especially crustose coralline algae (CCA), form a secondary group of carbonate producers (Payri, 1997). The physiochemical and biological lithification of carbonate forms an important third source. These sources of carbonate on reefs are offset by processes that erode the reef framework (Fig. 3). Violent tropical storms are natural events known to seriously affect coral reefs, but their frequency is low (Endean, 1976). The local breakage, toppling and overturning of corals caused by these events can set back reef growth for a century. In contrast to these natural phenomena, the process of bioerosion is a lot more frequent on coral reefs. First described by Neumann (1966), the term bioerosion involves any organism that erodes and weakens the calcareous skeletons of reef-building species. Numerous studies have shown that bioerosion plays an important role in sculpting coral reef growth and producing the sediments cement the structures of reef environments (Glynn & Manzello, 2015). Interestingly, carbonate budget studies have demonstrated that constructive and destructive processes are closely balanced on healthy reefs, with net reef accumulation only barely ahead of net reef loss (Glynn & Manzello, 2015; Glynn, 1988; Scoffin et al., 1980). Carbonate budgets allow for the conceptualization and quantification of coral reef growth in a time where environmental and ecological stressors are pervasive on reefs (Glynn & Manzello, 2015; Perry et al., 2012).

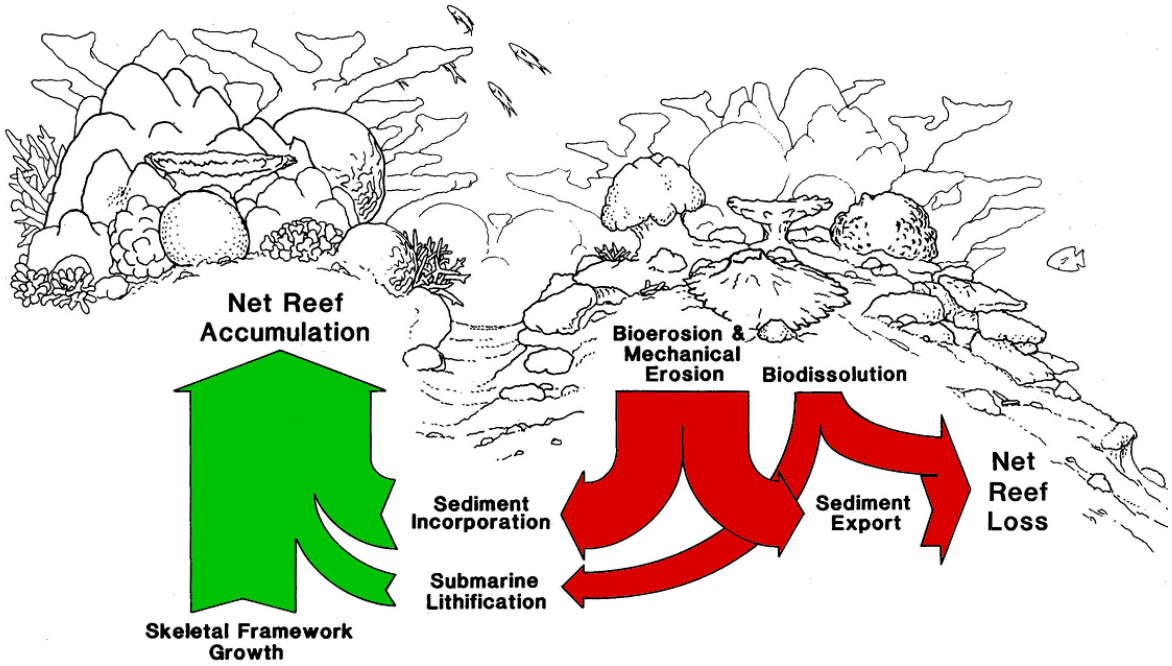

Fig. 3. The carbonate budget consists of a dynamic balance between reef production and erosion processes (green and red arrows resp.). Processes that lead to reef accumulation are offset by erosional processes, which can be destructive natural events such as tropical storms but also the action of bioeroding organisms that weaken the carbonate framework. Figure adapted from Glynn & Manzello (2015).

1.4 *Changing dynamics of Caribbean reefs*

Although coral reefs are declining globally, the state of Caribbean reefs is arguably the most alarming (Glynn & Manzello, 2015; Perry et al., 2013, 2014). Caribbean reefs have experienced several major disturbances that have led to large-scale coral mortality such as the ecological extinction of the keystone sea urchin herbivore *Diadema antillarum*, overfishing, coastal pollution, high seawater temperatures inducing coral bleaching (symbiont loss) and disease (Aronson & Precht, 2001; Eakin et al., 2010; Hughes, 1994; Jackson et al., 2001). Since the 1970s, live coral cover has declined by about 80% and carbonate production by corals has decreased to 50% below historical averages (Gardner et al., 2003; Perry et al., 2013). Caribbean reefs are not only losing their architectural complexity which is crucial to species diversity, but more than a third of investigated reef sites were found in net erosional states, displaying negative carbonate budgets (Alvarez-Filip et al., 2009; Perry et al., 2013). Field studies by Perry et al. (2013) suggest that a live coral cover threshold of ≥10% is crucial to maintain a positive carbonate budget. Since many Caribbean reefs exhibit live coral cover close to this value, it is likely that their carbonate budgets are in a neutral state, a phenomenon termed 'accretionary stasis' (Perry et al., 2008).

With most Caribbean reefs in accretionary stasis, shifts in the relative importance of the processes illustrated in Fig. 3 could define future carbonate budget trajectories (Perry et al., 2014). Because the compounded effects of ocean acidification and warming have significantly reduced reef-building potential (Fig. 3, green arrows) (Hoegh-Guldberg et al., 2007), shifts in erosional processes (Fig. 3, red arrows) could have substantial consequences for the carbonate budgets of coral reefs (Perry et al., 2014). A study by Kennedy et al. (2013) found that changes in coral calcification due to warming and ocean acidification were most important in carbonate budget simulations for healthy, coral-dominated reefs. Conversely, bioerosion became the dominant process in unhealthy reefs exhibiting low coral cover.

1.5 *Bioeroding sponges*

Widespread declines in coral coverage are known to facilitate increased bioeroder abundance (Carballo et al., 2013; Holmes, 2000; López-Victoria & Zea, 2004; Rose & Risk, 1985). Furthermore, increased bioerosion rates under acidification and/or warming scenarios have been reported for several taxa of bioeroders, including algae (Tribollet et al., 2009), polychaetes, lithophagid bivalves (DeCarlo et al., 2014) and sponges (Fang et al., 2013; Fang et al., 2014; Stubler et al., 2015; Wisshak et al., 2012, 2013). Sponges are the most effective group of bioeroders in terms of total carbonate mass removed from coral reefs (Neumann, 1966), ranging from 0.84 to up to 23 kg $CaCO_3$ m^{-2} $year^{-1}$, accounting for up to 95% of total bioerosion (Nava & Carballo, 2008; Zundelevich et al., 2007a). Specifically, sponges from the genus *Cliona* are the most common and destructive bioeroders on coral reefs worldwide (Glynn & Manzello, 2015; Schönberg, 2008). The potential of this significant group of bioeroders to shift reefs into a negative carbonate budget in the future is exacerbated by several factors: a) residing inside carbonate framework, their endolithic lifestyle provides shelter from predators and adverse

ambient conditions (Schönberg & Suwa, 2007), b) organic pollution (i.e. eutrophication) benefits these filter feeders (Holmes, 2000; Rose & Risk, 1985), c) they are highly opportunistic and resilient, showing major increases after bleaching events that damage and kill corals, thus allowing quick colonization of the newly available dead coral substrate (Carballo et al., 2013; Glynn & Manzello, 2015; Schönberg & Ortiz, 2008), and d) seawater temperature increases may promote their growth, increasing their bioerosion potential (Márquez et al., 2006; Rützler, 2002). Negative carbonate budgets as result of intensive sponge bioerosion have already been recognized on some reefs and may become pervasive under future climate scenarios (Acker & Risk, 1985; Enochs et al., 2015a; Nava & Carballo, 2008). The reaction of bioeroding sponges to the processes of ocean acidification and the lowering of oceanic Ω remains unknown.

1.6 *Shedding light on clionaid bioerosion*

Although the general process of clionaid bioerosion is known, the driving physiological and chemical mechanisms are only partly understood. It is known that calcium carbonate dissolution by sponges is accomplished by cells called amoebocytes which etch and chip away minute fragments of carbonate (Fig. 4), often referred to as 'sponge chips' (Pomponi, 1979; Rützler & Rieger, 1973). By dissolution of aragonite, the amoebocytes extend fine filopodia sheets into the carbonate that eventually meet each other, cutting out a hemispherical carbonate chip (Fig. 5, size range 15–85 µm). This chip production constitutes the mechanical boring of sponges; but the detachment of chips by amoebocytes from solid carbonate requires the use of chemical boring as well. The exact etching agent involved in chemical bioerosion remains unknown, but the enzymes carbonic anhydrase and acid phosphatase have been hypothesized to be involved in sponge bioerosion, providing means for mineral dissolution and the digestion of organic components (Schönberg, 2008). Once the sponge chips are produced, they are expelled from the sponge together with their associated etching cells. Paradoxically, sponge chips contribute up to 40% of carbonate sediments on Caribbean reefs (Glynn & Manzello, 2015), thus partially facilitating the sediment incorporation process that consolidates and strengthens reef structures (Perry et al., 2008) (Fig. 3).

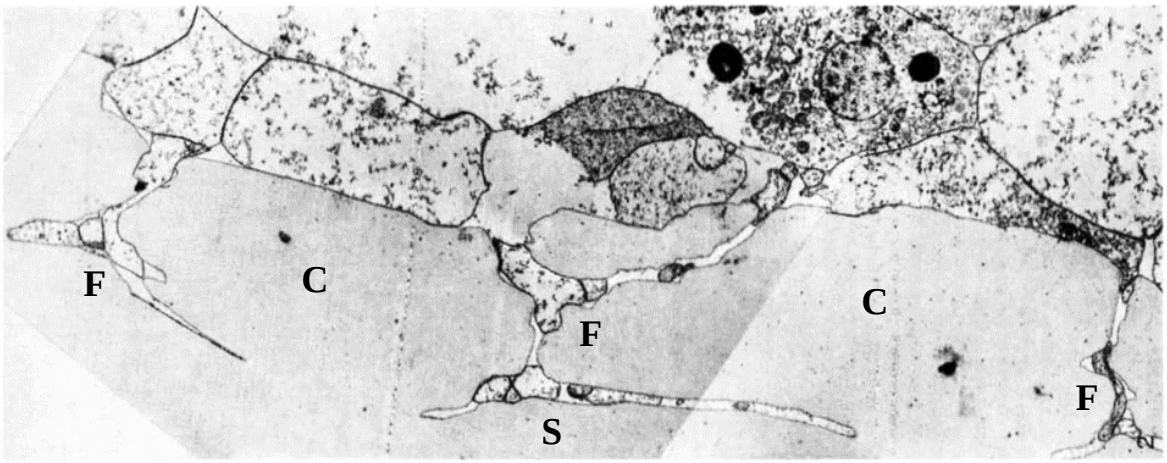

Fig. 4. Etching cells in cross section of *C. lampa* in the process of undercutting sponge chips (C) in the substratum (S). The etching cell filopodia (F) slowly burrow into the substratum until they meet, dislodging the carbonate and forming a sponge chip. (TEM, x2500) Image adapted from Rützler and Rieger (1973).

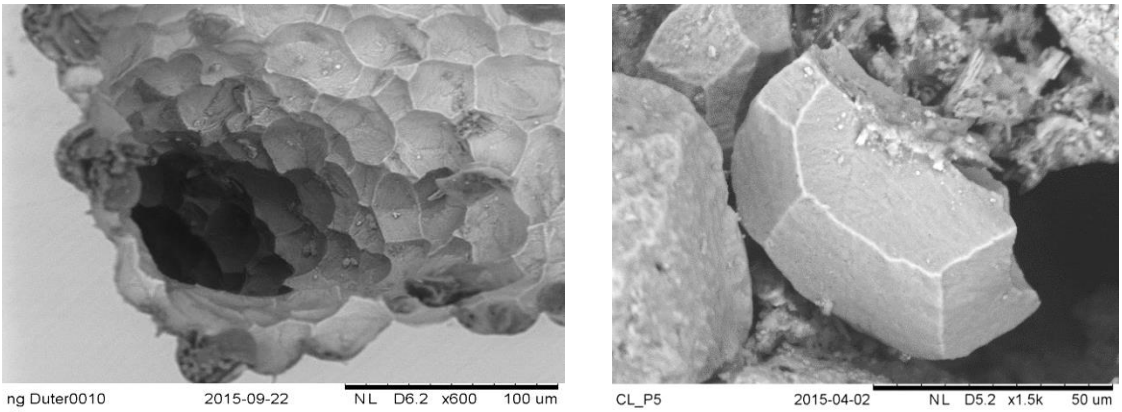

Fig. 5. Bioerosion by sponges leaves tell-tale concave chipping marks in the carbonate substrate. The left pane illustrates a piece of calcite (Icelandic spar) with extensive bioerosion marks. The proximity of these chip marks to each other causes distinct edges on the produced sponge chips (right pane).

Recent studies have found that clionaid bioerosion rates will very likely increase in a high-CO_2 world, possibly in synergy with elevated seawater temperatures (Enochs et al., 2015; Fang et al., 2013, 2014; Stubler et al., 2014, 2015; Wisshak et al., 2012, 2013). However, the effect of temperature may actually cause a parabolic response, whereby bioerosion rates could increase up to a certain thermal threshold and then decline due to the clionaid sponges experiencing an overall negative energy balance as a result of metabolic costs (Fang et al., 2014). Similar parabolic temperature responses were reported by Wisshak et al. (2013) and Enochs et al. (2015) and may also be linked to disease and/or bleaching in symbiont-bearing clionaid sponges (Schönberg et al., 2008; Schönberg, 2008).

Despite the forecasted enhanced clionaid bioerosion under future climate scenarios, it is still unknown which component(-s) of the carbonate system is actually impacting coral aragonite loss. The increase in $[H^+]$ due to ocean acidification has generally been attributed to facilitate increased sponge bioerosion rates by decreasing $[CO_3^{2-}]$, lowering the environmental threshold for substrate dissolution (i.e. Ω). A lower Ω would decrease the metabolic cost of chemical bioerosion, subsequently increasing the efficiency of the bioerosion process and leading to significantly increased sponge bioerosion rates (Fang et al., 2013; Wisshak et al., 2012). This hypothesis poses a clear link between $[H^+]$ and $[CO_3^{2-}]$ in the bioerosion process, since the inverse covariance of these two ions is an intrinsic part of the carbonate system. However, the underlying mechanisms driving bioerosion and how they are affected by ocean acidification have not yet been studied in detail and there is currently no proposed model for sponge bioerosion.

Here, we will try to verify the link between $[H^+]$ and $[CO_3^{2-}]$ proposed by these previous workers. By decoupling the covariance of $[H^+]$ and $[CO_3^{2-}]$, we aim to reveal the individual effects of these parameters on sponge bioerosion rates. Experimentally varying one of these two parameters at a time whilst keeping the other constant will enable us to shed light on the possible mechanisms responsible for the enhanced bioerosion rates associated with ocean acidification.

2. Methods

2.1 Study location

All sampling and experimental work was conducted on the island of St. Eustatius, Dutch Caribbean (Fig. 6, left). A leeward fringing reef in Gallows Bay was selected as the sampling site for specimens within the sponge *Cliona caribbaea* (Fig. 4, right, marked by an asterisk, *).

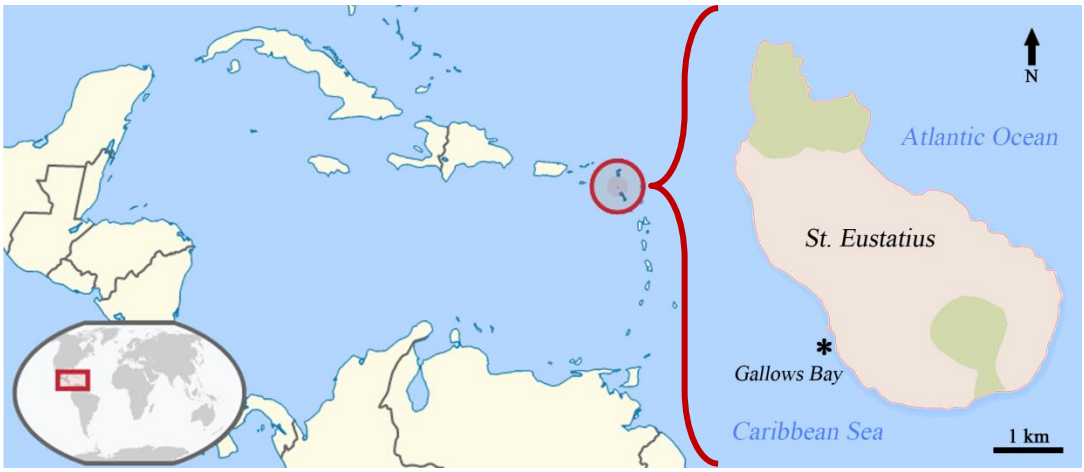

Fig. 6. The location of St. Eustatius in the Caribbean (left) and the sampling site on the leeward fringing reef in Gallows Bay (right). Figure adapted from Wikipedia Commons and Google Maps.

2.2 Sponge collection

At this reef, the symbiont-bearing sponge species *C. caribbaea* was core-sampled in 1 to 3 m water depth from large overgrown *Diploria labyrinthiformis* (grooved brain coral) colonies with an air-drill and hole-saw (inner diameter: 30 mm, Fig. 7, left). Cores containing only carbonate were also drilled and used as control cores. Each sponge core sample (n = 20) contained sponge-infested material in the upper section and clean coral skeleton below (Fig. 7, right). The core samples were color coded and transferred into outdoor flow-through tanks under ambient conditions for a week to allow the sponge tissue to fully heal before starting the experiment.

Fig. 7. Core-sampling of a *D. labyrinthiformis* colony overgrown by *C. caribbaea* (left). The resulting sponge cores were allowed to fully heal before the start of the experiment (right).

***2.3** Incubation scenario preparations*

To experimentally vary $[H^+]$ or $[CO_3^{2-}]$ whilst keeping the other parameter constant, four batches of chemically altered seawater were prepared from one initial batch of seawater (Table 1). This involved carefully adjusting two properties, dissolved inorganic carbon (DIC) and total alkalinity (A_T). The definitions of DIC and the total alkalinity of seawater are given by equations 6 and 7 respectively (Dickson et al., 2007; Stumm & Morgan, 1981):

$$DIC = [CO_2^*] + [HCO_3^-] + [CO_3^{2-}] \quad (6)$$

$$A_T = [HCO_3^-] + 2[CO_3^{-2}] + [B(OH)_4^-] + [OH^-] - [H^+] \quad (7)$$

whereby $[CO_2^*]$ describes dissolved $[CO_2]$ and $[H_2CO_3]$ in water. A_T is defined as the excess of proton acceptors over proton donors (Wolf-Gladrow et al., 2007) and is a key property of the inorganic carbon system. DIC and A_T were manipulated in three ways: 1) by addition of $NaHCO_3$ and/or Na_2CO_3 to increase A_T and DIC in a ratio of 1:1 and 2:1 respectively, 2) addition of 0.1M HCl to decrease A_T while keeping DIC constant, and 3) addition of HCl to decrease A_T in combination with purging by N_2 gas to decrease DIC. The pre- and post-treatment A_T and DIC of the batches were measured using a Versatile Instrument for the Determination of Titration Alkalinity (VINDTA) (Mintrop et al., 2000) at the Caribbean Netherlands Science Institute (CNSI), the remaining components of the carbonate system were calculated using the CO2SYS program (Table 2; Pierrot et al., 2006). The accuracy and precision of the VINDTA measurements was ±4 and ±2 for T_A, ±1 and ±5 for DIC respectively.

Table 1. Four batches reflecting different chemical scenarios were prepared by adjusting DIC and TA accordingly.

Scenario	*Variable*	*Constant*	*Chemical(s) and/or process used*
1	High $[CO_3^{2-}]$	pH	$NaHCO_3$, Na_2CO_3
2	Low pH	$[CO_3^{2-}]$	$NaHCO_3$, HCl
3	Low $[CO_3^{2-}]$	pH	HCl, N_2 purging
4	Low $[CO_3^{2-}]$ * Low pH	-	HCl, N_2 purging

Table 2. Chemical compositions of the four batches in relation to initial values. *N* denotes control conditions.

Scenario	A_T	DIC	pH	$[HCO_3^-]$	$[CO_3^{2-}]$	Ω
N	2333.6	2005.9	8.034	1761.7	233.6	3.77
1	5612.8	4953.7	8.04	4347.36	580.36	9.37
2	5261	5033.1	7.64	4711.8	250.63	4.04
3	1060	870.4	8.01	769.83	95.63	1.54
4	1292.4	1205.8	7.62	1130.31	57.88	0.93

***2.4** Chemical bioerosion rates*

Rates of chemical bioerosion (kg $CaCO_3$ m^{-2} $year^{-1}$) were calculated from the change in A_T during day and night incubation periods of varying length. Using the incubation method, the change in A_T (ΔA_T) in each incubation chamber is almost entirely the result of $CaCO_3$ production or - dissolution, with the impact of respiration and photosynthesis on A_T considered negligible in our calculations (Zundelevich et al., 2007). Since A_T increases with dissolution and decreases with calcification, the equation shows that the molar amount of $CaCO_3$ dissolved by the bioeroding sponges was half of the observed A_T increase in the incubation chamber. ΔA_T was calculated for each chamber by subtracting the A_T at the end of each incubation from the initial A_T. A_T and DIC were determined using the VINDTA. The mass of $CaCO_3$ dissolved by the bioeroding sponges, $m_{(CaCO_3)}$ (in g) was calculated from ΔA_T by:

$$m_{(CaCO_3)} = 0.5\ (\text{mol eq}^{-1}) \times \Delta A_T \times 100 \times V_{sw} \times \rho_{sw} \qquad (8)$$

where 100 is the molar mass of $CaCO_3$; V_{sw} is the volume (in l) of seawater in the incubation chamber; and ρ_{sw} seawater density (Zundelevich et al., 2007). Subsequently relating the mass of $CaCO_3$ dissolved by the bioeroding sponges to the sponge tissue surface area determined from measurements and photographs, final sponge bioerosion rates were calculated and converted to [kg $CaCO_3$ m^{-2} $year^{-1}$]. This allowed for ecologically relevant comparisons with published literature regarding reef carbonate budgets (e.g. census-based approaches by Perry et al. (2012)).

***2.5** Mechanical bioerosion rates*

The methods used to quantify the aragonite chips produced by the bioeroding sponges during incubation follows Fang et al. (2013). After extracting most of the incubation chamber water for chemical bioerosion rate analysis, the remaining volume (containing the sponge chips) were filtered through a 150 µm sieve to remove coarser materials and subsequently filtered through a 0.7 µm GF/F glass microfiber filter paper which was precombusted at 550 °C for 3h and pre-weighed. Each chamber was given a final rinse with 200 ml distilled water that was run through the same filter to recover the remaining sponge chips. The filter was then again combusted at 550 °C for 3h to remove organic matter and reweighed, thus allowing calculation of the sediment weight produced over the incubation period. The weight of sediment obtained from 250 ml was multiplied by 2 to correct for the 500 ml final volume. Previous authors (e.g. Fang et al., 2013; Zundelevich et al., 2007) have calculated mechanical bioerosion rates directly from this weight difference, assuming that the sediment on the filters can be attributed to the presence of sponge chips. We used scanning electron microscopy (SEM) analysis of our filters to verify this assumption. On filters from both day and night incubations, diagonal transects of 5-10 images at 300x magnification from both the middle and outer areas of each filter were captured and analyzed for sponge chip presence and quantity. Unlike previous studies, we did not filter our treatment water prior to incubations so that DIC levels would remain similar to the control (*N*) scenario. Thus, the filters did contain single-celled organisms but their overall biomass was

considered negligible in comparison to sponge chip numbers. A SEM image used in the analysis is given in Fig. 8 as an example.

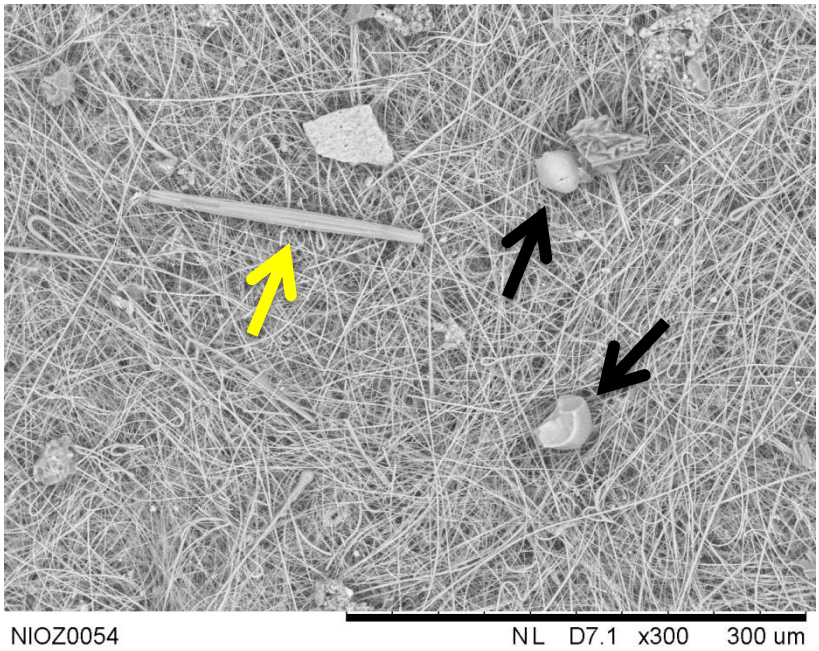

Fig. 8. An example SEM image containing two sponge chips and a single-celled organism (black and yellow arrows resp.)

2.6 *Incubation rounds*

Over an interval of two days, four rounds of incubations were performed, spanning both the night and day (Table 3, next page). Preliminary testing showed a significant difference in oxygen levels after day and night incubations. Night incubations with durations longer than 3 hours suffered from substantial oxygen depletion due to the absence of photosynthesis and possibly increased respiration rates. A duration of 3 hours was subsequently chosen for the night incubations. Photosynthesis during day incubations yielded unaltered oxygen levels, thus allowing for a longer incubation duration of 6 hours. The day and night incubations were started at ecologically relevant time points, i.e. at daybreak and sundown respectively. This also allowed the sponges to recover between incubations. Material limitations during the making of the batch for scenario 4 resulted in a lower end volume than expected, allowing for just one day incubation (Table 3).

Table 3. Arrangement of the incubation rounds performed over two consecutive days. *N* denotes control conditions.

Incubation round	*Scenario(s)*	*Time of day*	*Duration (h)*
1	1, 4	Day	6
2	*N*, 2, 3	Night	3
3	*N*, 2, 3	Day	6
4	1	Night	3

The incubation chambers were custom designed and fabricated at the NIOZ to accommodate 500 ml of treatment water and a magnetic stirrer to stimulate water circulation during incubation (Fig. 9). Each incubation chamber contained 2 cores per round and each scenario contained a control core with no sponge tissue as a control for passive dissolution. Chambers were placed in an array alongside their respective tanks, filled with the appropriate scenario water and sponge cores. Each chamber contained a minimal headspace to prevent gas exchanges effecting the water chemistry. At the start of each incubation round, the magnetic stirrers were activated simultaneously and kept on for the duration of the incubation. At incubation completion, the top lids were carefully removed and the chamber water was transferred into alkalinity bottles with large plastic syringes for chemical bioerosion analysis. The cores were then rinsed with the remaining chamber water to ensure all sponge chips were flushed to the bottom of the chamber. After returning the cores to their respective tanks, the remaining chamber water was transferred into falcon tubes to recover the sponge chips.

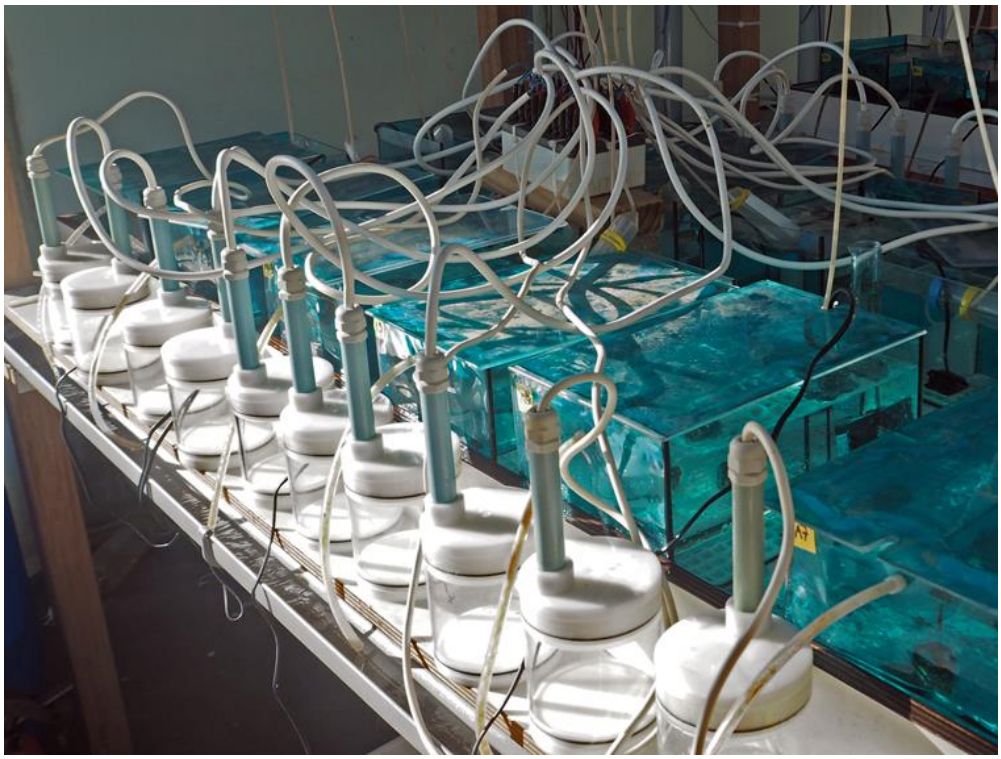

Fig. 9. Incubation chamber set up. The protruding structures are magnetic stirrers.

3. Results

3.1 Chemical bioerosion rates

3.1.1 Incubation results

The final incubation results are given in Table 4. By subtracting final by initial alkalinities and DIC ($T_{A\ final} - T_{A\ initial}$ and $DIC_{final} - DIC_{initial}$), the change (Δ) of these two parameters during incubation was calculated. Given the 2:1 relation between T_A and DIC, the DIC change due to bioerosion ($DIC_{bioerosion}$) is given by ($T_{A\ final} - T_{A\ initial}$)/2. The change in DIC due to metabolic processes was then calculated via DIC_{total} - $DIC_{bioerosion}$, yielding $DIC_{metabolism}$. We assumed this residual DIC change to reflect respiration and photosynthesis processes. All Δ values were subsequently normalized for incubation duration (6h for day, 3h for night) and sponge tissue/control core area (cm^2).

3.1.2 Chemical bioerosion incubation results

Scenarios *N*, 3 and 4 showed positive bioerosion rates, whereas scenarios 1 and 2 resulted in negative bioerosion rates, indicating carbonate accretion (Table 5, Fig. 10). The highest bioerosion rates were found in scenarios 3 and 4, whereas accretion was highest in scenario 1. Overall, bioerosion and accretion rates were higher during night incubations than day incubations. The absence of a night incubation for scenario 4 only makes it impossible to compare rates between day and night at low [CO_3^{2-}] in combination with a low pH. The control cores consistently yielded results different from the sponge cores exposed to the same treatment scenario.

Table 4. Incubation results. Differences (Δ) in TA and DIC after incubation were calculated in relation to initial conditions and normalized for incubation duration (6h for day, 3h for night) and sponge tissue/control core area (cm²). The components of DIC due to bioerosion and metabolism and their ratio were subsequently calculated. Negative values for these two DIC parameters indicate accretion and photosynthesis respectively, whereas positive values indicate bioerosion and respiration.

Scenario description	*Incubation (day/night)*	*Core type*	*Area (cm²)*	T_A	*DIC*	*Norm. ΔT_A*	*Norm. ΔDIC*	*Norm. ΔDIC bioerosion*	*Norm. ΔDIC metabolism*	*Ratio norm. bioerosion/ metabolism*
Normal	D	initial	-	2333.61	2005.88	-	-	-	-	-
Normal	D	control	25	2305.12	1827.11	-0.19	-1.19	-0.09	-1.10	0.09
Normal	D	sponge	36.4	2365.57	2019.73	0.15	0.06	0.07	-0.01	-7.51
Normal	D	sponge	42	2384.00	2095.21	0.20	0.35	0.10	0.25	0.40
Normal	N	initial	-	2338.64	2022.89	-	-	-	-	-
Normal	N	control	25	2336.91	2021.19	-0.02	-0.02	-0.01	-0.01	1.03
Normal	N	sponge	42	2360.41	2140.12	0.17	0.88	0.09	0.79	0.11
High [CO_3^{2-}]	D	Initial	-	5612.79	4953.69	-	-	-	-	-
High [CO_3^{2-}]	D	control	25	5223.24	4752.13	-2.60	-1.34	-1.30	-0.05	28.74
High [CO_3^{2-}]	D	sponge	40	5133.79	4436.91	-2.00	-2.15	-1.00	-1.16	0.86
High [CO_3^{2-}]	D	sponge	39.8	5077.08	4319.41	-2.24	-2.66	-1.12	-1.53	0.73
High [CO_3^{2-}]	N	initial	-	5731.11	5036.68	-	-	-	-	-
High [CO_3^{2-}]	N	control	25	5351.84	4772.66	-5.06	-3.52	-2.53	-0.99	2.55
High [CO_3^{2-}]	N	sponge	39.8	5327.90	4820.47	-3.38	-1.81	-1.69	-0.12	13.81
Low pH	D	initial	-	5261.03	5033.08	-	-	-	-	-
Low pH	D	control	25	5106.20	4740.54	-1.03	-1.95	-0.52	-1.43	0.36
Low pH	D	sponge	30.2	4908.47	4314.25	-1.95	-3.97	-0.97	-2.99	0.32
Low pH	D	sponge	35.2	5002.79	4556.22	-1.22	-2.26	-0.61	-1.65	0.37
Low pH	N	initial	-	5276.95	5008.59	-	-	-	-	-
Low pH	N	control	25	5097.62	4432.65	-2.39	-7.68	-1.20	-6.48	0.18
Low pH	N	sponge	30.2	5087.46	4906.18	-2.09	-1.13	-1.05	-0.08	12.36
Low pH	N	sponge	35.2	5038.54	4864.30	-2.26	-1.37	-1.13	-0.24	4.75
Low [CO_3^{2-}]	D	initial	-	1066.42	934.90	-	-	-	-	-
Low [CO_3^{2-}]	D	sponge	39.5	1270.90	1054.52	0.86	0.50	0.43	0.07	5.88
Low [CO_3^{2-}]	D	sponge	35.2	1252.09	886.57	0.88	-0.23	0.44	-0.67	0.66
Low [CO_3^{2-}]	N	initial	-	1059.96	834.17	-	-	-	-	-
Low [CO_3^{2-}]	N	sponge	39.5	1208.99	1239.45	1.26	3.42	0.63	2.79	0.23
Low [CO_3^{2-}]	N	sponge	35.2	1173.62	1023.37	1.08	1.79	0.54	1.25	0.43
Low [CO_3^{2-}] & low pH	D	initial	-	1139.97	1367.01	-	-	-	-	-
Low [CO_3^{2-}] & low pH	D	control	25	1050.10	1114.64	-0.60	-1.68	-0.30	-1.38	0.22
Low [CO_3^{2-}] & low pH	D	sponge	39.5	1514.22	1467.49	1.58	0.42	0.79	-0.37	-2.16
Low [CO_3^{2-}] & low pH	D	sponge	35.2	1431.02	1416.22	1.38	0.23	0.69	-0.46	-1.51

Table 5. Chemical bioerosion analysis results. Chemical bioerosion rates were calculated for both sponge and control cores by measuring the change in T_A and applying equation 2 (methods section). Positive values indicate an increase in T_A and thus a mass change due to sponge bioerosion, whereas negative values indicate accretionary processes. The average chemical bioerosion rate is given for the sponge cores of each scenario ± standard deviation.

Scenario	*Description*	*Incubation (day/night)*	*Core type*	*Bioerosion rate (kg m^{-2} year^{-1})*	*Average chem. bioerosion rate*
N	Normal	D	control	-0.43	
N	Normal	D	sponge	0.33	0.39 ± 0.06
N	Normal	D	sponge	0.46	
N	Normal	N	control	-0.05	
N	Normal	N	sponge	0.39	0.39 ± 0.00
1	High [CO_3^{2-}]	D	control	-5.82	
1	High [CO_3^{2-}]	D	sponge	-4.47	-4.75 ± 0.28
1	High [CO_3^{2-}]	D	sponge	-5.03	
1	High [CO_3^{2-}]	N	control	-11.34	
1	High [CO_3^{2-}]	N	sponge	-7.57	-7.57 ± 0.00
2	Low pH	D	control	-2.31	
2	Low pH	D	sponge	-4.36	-3.55 ± 0.81
2	Low pH	D	sponge	-2.74	
2	Low pH	N	control	-5.36	
2	Low pH	N	sponge	-4.69	-4.88 ± 0.19
2	Low pH	N	sponge	-5.06	
3	Low [CO_3^{2-}]	D	sponge	1.93	1.95 ± 0.02
3	Low [CO_3^{2-}]	D	sponge	1.97	
3	Low [CO_3^{2-}]	N	sponge	2.82	2.62 ± 0.20
3	Low [CO_3^{2-}]	N	sponge	2.41	
4	Low [CO_3^{2-}] & low pH	D	control	-1.34	
4	Low [CO_3^{2-}] & low pH	D	sponge	3.54	3.31 ± 0.23
4	Low [CO_3^{2-}] & low pH	D	sponge	3.09	

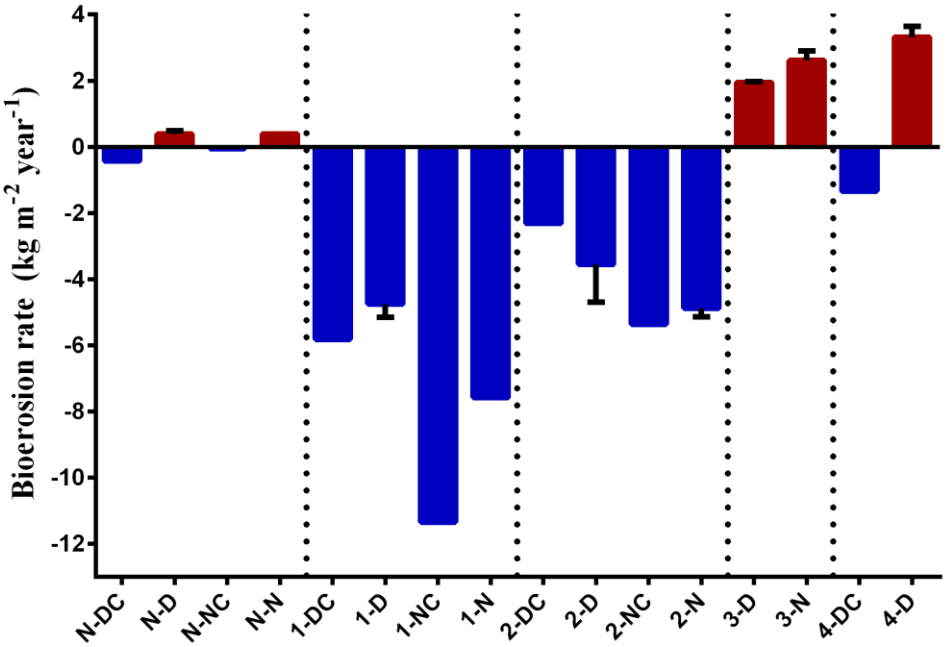

Fig. 10. Bar plot of Table 5. Positive rates (bioerosion) are indicated in red, negative rates (accretion) in blue. Labels start with scenario codes found in Table 5, after which day (D), night (N) and control core (C) are indicated. Error bars indicate standard deviation.

3.1.3 *Correlations with chemical bioerosion rates*

Cross-correlations were performed between the calculated chemical bioerosion rates and selected carbonate system parameters using the Pearson product-moment method (Table 6). With the exception of pH, all parameters were significantly correlated with chemical bioerosion rates for the sponge cores. The significance of each correlation was similar between day and night incubations for all parameters except [CO_3^{2-}]. None of the correlations calculated for the control cores were significant. All significant correlations with exception of $DIC_{metabolism}$ were negative, displaying inversely proportionate relations.

Table 6. Correlation results using the Pearson product-moment method. Correlations were performed between the chemical bioerosion rate and relevant carbonate system variables.

	Sponge cores		**Control cores**	
	Day	Night	Day	Night
pH	-0.33	0.58	-0.32	-0.11
[HCO_3^-]	-0.95**	-0.96**	-0.70	-0.80
[CO_3^{2-}]	-0.87**	-0.87*	-0.88	-0.93
Ω	-0.95**	-0.87**	-0.88	-0.93
$DIC_{metabolism}$	0.74*	0.87*	-0.85	0.11
* indicates significance at α = 0.05, ** indicates significance at α = 0.01				

3.1.4 *Chemical bioerosion plots*

Chemical bioerosion rates were plotted against pH, Ω and $DIC_{metabolism}$ to visualize the data (Fig. 11a-11c). The parameter pH serves as an indirect measure of pCO_2, whereby a high pH coincides with a low pCO_2 and vice versa. The parameter Ω is directly related to [CO_3^{2-}], whereas [HCO_3^-] was not experimentally varied.

It is important to note that water chemistry change is a process inherent of incubations. Thus, even though all complementary incubations per scenario started with very similar chemical properties, these properties were subject to change throughout the incubations. Because we could not assume that the chemistry change during incubation was a linear process, averaging the initial and final incubation water properties would have been inaccurate in reflecting the exact water chemistry to which the cores were exposed. Furthermore, variations in sponge tissue mass and surface area also affect this response, altering the extent of chemistry change per incubation chamber. For these reasons, bioerosion rates are presented in relation to known initial incubation values of the assessed carbonate parameters (Table 2).

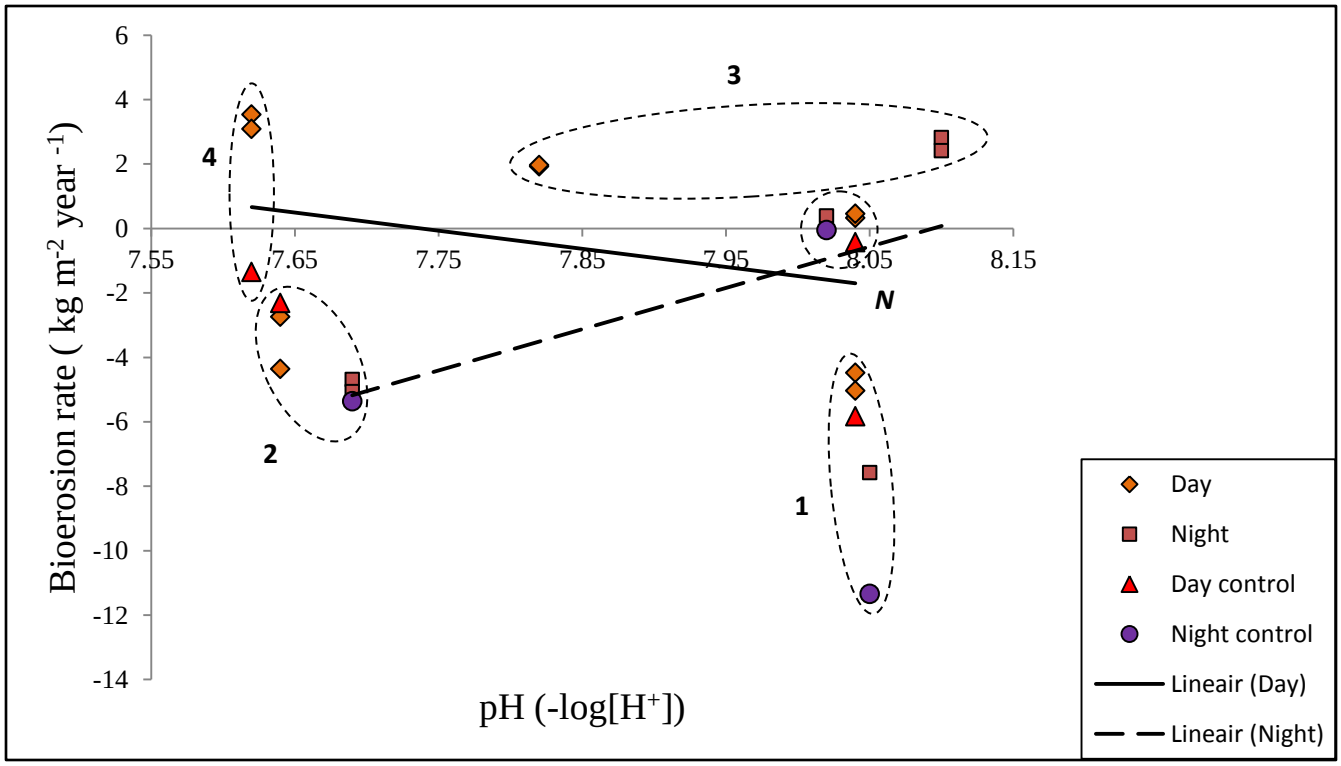

Fig. 11a. Initial pH conditions per scenario plotted against their respective chemical bioerosion rates. Data points are grouped by ovals (striped) with corresponding scenario codes (see Table 5).

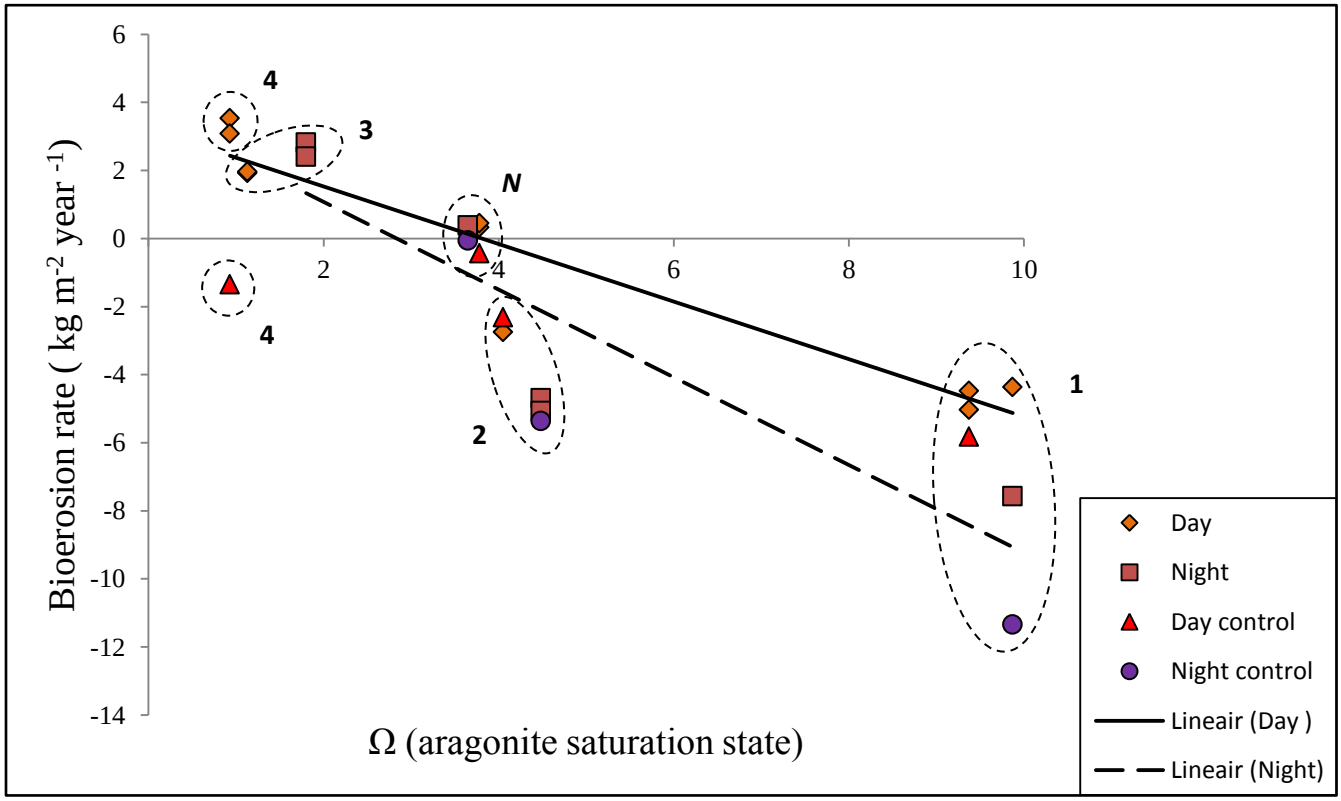

Fig. 11b. Initial Ω conditions per scenario plotted against their respective chemical bioerosion rates. Data points are grouped by ovals (striped) with corresponding scenario codes (see Table 5).

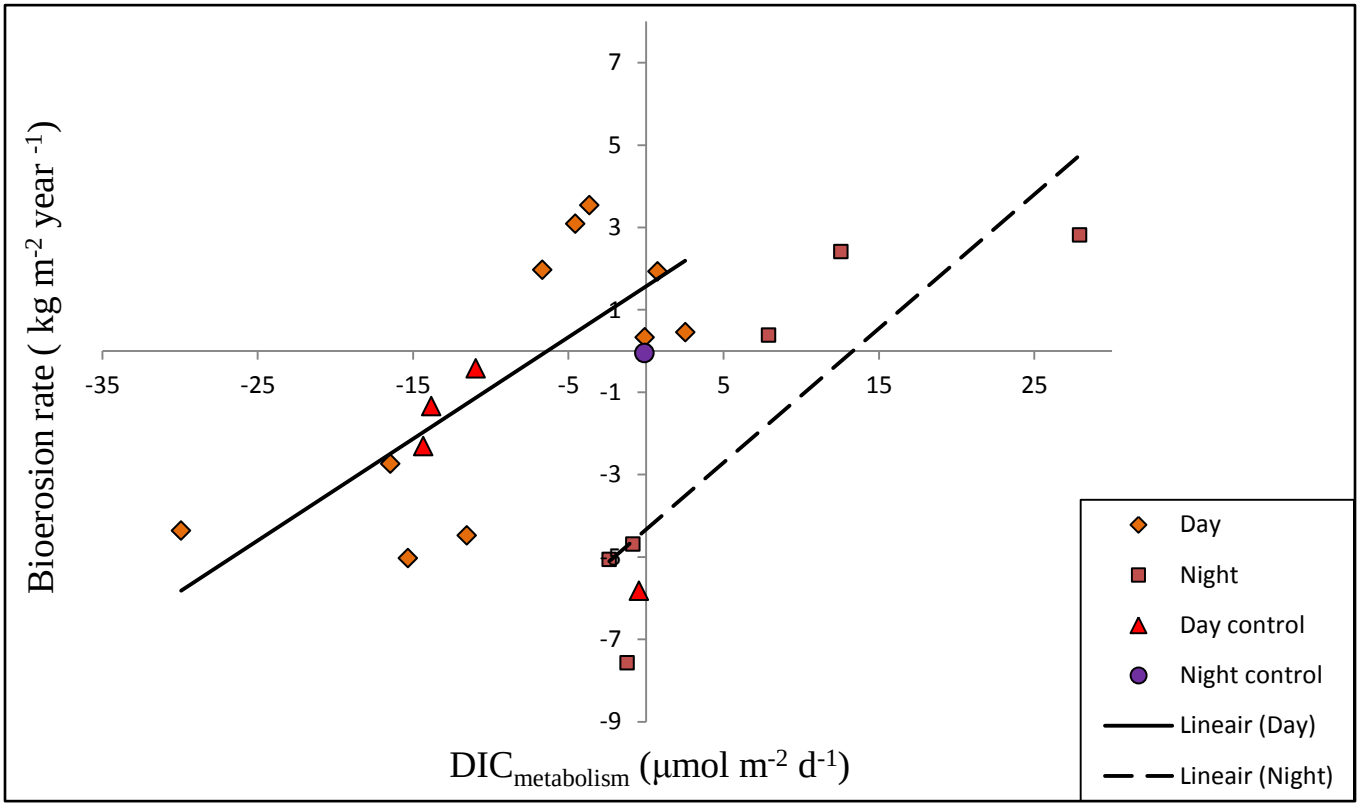

Fig. 11c. Initial $DIC_{metabolism}$ conditions per scenario plotted against their respective chemical bioerosion rates.

3.1.5 Parameters influencing chemical bioerosion rates

pH

There were no significant correlation between pH and chemical bioerosion rates (Table 6; Fig 11a). However, there was some effect given the observation that the relation between pH and bioerosion is opposite when comparing day and night. Decreased pH conditions resulted in increased bioerosion rates during the day, whereas increased pH conditions resulted in increased bioerosion rates during the night. Scenario 3 initial values varied more than intended, but night bioerosion rates were still higher than day rates despite a 51% decrease in $[H^+]$.

Ω

The significant correlations between Ω and chemical bioerosion rates (Table 6) display a clear trend; higher Ω leads to lower bioerosion/higher accretion rates. The contrast between day and night incubations was highest in scenario 3, whereby night conditions (for both sponge and control cores) yielded higher accretion rates than day incubations (e.g. scenario 1 and 2). Under low pH, $[CO_3^{2-}]$ and Ω conditions, the control core in scenario 4 did not reveal passive dissolution to be present. Given that this control core was exposed to the lowest Ω, we assumed passive dissolution to have been non-existent in the rest of the sponge and control cores.

$DIC_{metabolism}$

Not all day incubations showed DIC decreases that were expected via photosynthesis, with some being near net equilibrium/net respiration. Not all night incubations were in net respiration. Control cores during day incubations all showed $DIC_{metabolism}$ decreases, possibly indicating photosynthesis by endolithic algae. The highest respiration rates at night coincided with the highest bioerosion rates. The highest overall bioerosion rates coincided with the day incubations of scenario 4.

3.2 *Mechanical bioerosion rates*

The incubation results for mechanical bioerosion rates did not yield significantly different rates between incubation scenarios (Table 7, Fig. 12). However, the night incubation in the Normal scenario showed disproportionally high mechanical bioerosion. Sponge chip production was not measured for scenario 4 due to loss of sample water after sampling for chemical bioerosion. Sponge chip production was not measured for the control cores because sponge tissue was absent on these cores, and thus sponge chip production was not expected. Night incubations yielded higher mechanical bioerosion rates than day incubations. Highest mechanical bioerosion rates were observed in scenarios *N* and 3, whereas the lowest rates were found in scenario 1. The fraction of mechanical bioerosion contributing to total bioerosion rate (chemical + mechanical) varied considerably, ranging from -1 to 27% for day incubations and -2 to 74% for night incubations (Table 7). The highest contribution of mechanical bioerosion to the total bioerosion rate was seen in scenario *N*, although the disproportionate night incubation result may indicate a methodological error in sponge chip collection or filter weighing (Fig. 12).

Table 7. Mechanical and total bioerosion results. Mechanical bioerosion rates were calculated for sponge cores only by filtering remaining incubation chamber water and measuring the weight difference. The average mechanical bioerosion rate is given for the sponge cores of each scenario ± standard deviation. With mechanical bioerosion rates known, total rates and the contribution of mechanical bioerosion to the total bioerosion rate could be calculated. Where chemical or mechanical bioerosion rate data was unavailable, n/a values were produced because total and contribution values could not be calculated.

Scenario	*Description*	*Incubation (day/night)*	*Bioerosion rate (kg m^{-2} $year^{-1}$)*	*Average mech. bioerosion rate*	*Total bioerosion rate (mech.+chem.)*	*Contribution of mech. to total (%)*
N	Normal	D	0.12	0.11 ± 0.01	0.45	27
N	Normal	D	0.10		0.56	19
N	Normal	N	0.16	0.64 ± 0.48	n/a	n/a
N	Normal	N	1.11		1.50	74
1	High [CO_3^{2-}]	D	0.04	0.05 ± 0.02	-4.44	-1
1	High [CO_3^{2-}]	D	0.07		-4.96	-1
1	High [CO_3^{2-}]	N	0.07	0.07 ± 0.00	n/a	n/a
1	High [CO_3^{2-}]	N	n/a		n/a	n/a
2	Low pH	D	0.10	0.09 ± 0.01	-4.27	-2
2	Low pH	D	0.08		-2.66	-3
2	Low pH	N	0.10	0.09 ± 0.01	-4.59	-2
2	Low pH	N	0.08		-4.98	-2
3	Low [CO_3^{2-}]	D	0.11	0.14 ± 0.03	2.05	5
3	Low [CO_3^{2-}]	D	0.17		2.14	8
3	Low [CO_3^{2-}]	N	0.30	0.27 ± 0.02	3.11	9
3	Low [CO_3^{2-}]	N	0.25		2.66	9

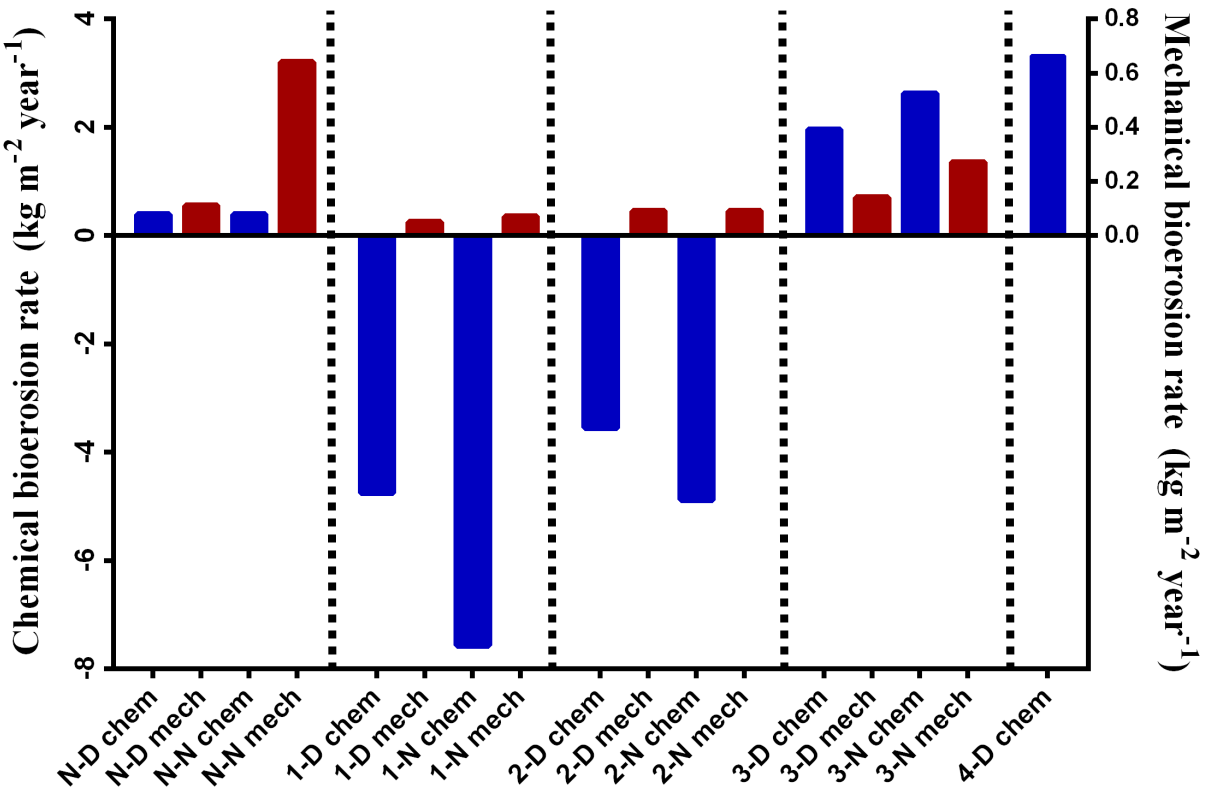

Fig. 12. Bar plot of Table 7. Chemical bioerosion (chem) is indicated in blue, mechanical bioerosion (mech) in red. Labels start with scenario codes found in Table 7, after which day (D) or night (N) are indicated.

3.3 Oxygen measurements

The oxygen contents after incubation completion were measured with a oxygen sensor (Walz, Germany) for a subset of the samples to get an indication of oxygen dynamics during the day and night incubations. The day incubations for the sponge cores resulted in oxygen levels (% ± SD) of 29.13 ± 6.38, whereas coinciding night incubations yielded 12.45 ± 0.72. The average change from initial conditions (21%) for the sponge core day incubations was 8.13 ± 6.38 and -8.55 ± 0.72 during the night. The day incubations for the control cores resulted in oxygen levels of 25.40 ± 0.00 and 18.33 ± 0.26 during the night. The average change from initial conditions for the control core day incubations was 4.40 ± 0.00 and -2.67 ± 0.26 during the night. Day incubations yielded higher than initial oxygen concentrations due to photosynthesis, whereas night incubations showed a gradual reduction in oxygen content due to respiration processes. The change from initial oxygen conditions was 2 to 4 times greater in sponge cores than in control cores.

4. Discussion

4.1 Overall results

The results showed strong variations in chemical bioerosion rates between the experimental conditions, whereas mechanical bioerosion remained similar. In this experiment, bioerosion rates were most strongly related with [CO_3^{2-}] and thereby, Ω. Bioerosion rates were highest at the lowest carbonate ion concentrations and saturation states. Conversely, accretion rates were highest at the highest carbonate ion concentrations and saturation states. Manipulation of pH (i.e. [H^+]) did not result in increased bioerosion rates, nor did it relate to net accretion rates.

4.2 Chemical bioerosion rates

4.2.1 The effect of the treatments

All control cores showed mild accretion rates, possibly reflecting the presence of calcifying endolithic algae. The control core in scenario 4 was the only one subjected to Ω <1 (Table 2, Fig. 11b) but still showed net accretion. We therefore assumed that any non-biological dissolution is negligible in comparison to the dissolution by the sponges.

Scenario 4 was the only manipulated scenario that reflected the natural covariance of [CO_3^{2-}] and [H^+], reflecting an extreme ocean acidification scenario (i.e. high atmospheric CO_2). Under both low [CO_3^{2-}] and high [H^+] (low pH) conditions, bioerosion rates approached values about 8.5 times higher than in the chemically unaltered conditions of scenario *N* (Table 5). Given that our results showed enhanced bioerosion rates (34% higher) during night incubations of scenario 3 compared to day incubations, a night incubation under scenario 4 may well have resulted in the highest bioerosion rates.

The individual impacts of [CO_3^{2-}] and [H^+] (i.e. comparing scenarios 2 and 3) suggest that the latter of the two has little impact on (chemical) bioerosion rates. The high [H^+] conditions of scenario 2 (an approximate 250% increase in [H^+] compared to control conditions) did not result in enhanced bioerosion (Table 5). Instead, accretion rates were comparable to those found in the field (Perry et al., 2012). Conversely, the low [CO_3^{2-}] conditions of scenario 3 (an approximate 52 to 70% decrease in [CO_3^{2-}] compared to the control) resulted in bioerosion rates 5 to 6.7 times higher than in scenario *N* during day and night, respectively. Night bioerosion rates were 34% higher than the day incubations of scenario 3, suggesting a major effect of the absence of photosynthesis/increased respiration rates on bioerosion rates.

The enhanced bioerosion seen in scenario 4 with respect to scenario 3 (Table 5) indicates that increased bioerosion rates due to low [CO_3^{2-}] can be augmented even further by the presence of high [H^+]. High [H^+] alone is insufficient to induce bioerosion (Fig. 10) whereas low [CO_3^{2-}] resulted in elevated bioerosion rates. Thus, the decoupling of [CO_3^{2-}] and [H^+] in our experiment

suggests that [CO_3^{2-}] in particular (and thereby Ω) determines bioerosion rates, whereas [H^+] may add to this forcing. Given the high bioerosion rates in scenario 4, our results concur with the current hypothesis that bioerosion rates will increase under future climate change scenarios (Enochs et al., 2015; Fang et al., 2013; Glynn & Manzello, 2015; Hoegh-Guldberg et al., 2007; Stubler et al., 2015; Wisshak et al., 2012, 2013).

4.2.2 *Day/night differences in bioerosion rates*

Night bioerosion rates are ~34% higher than those during the day (Table 5, Fig. 10). It is likely that this difference is driven by photosynthesis and respiration influencing the water chemistry and physiology within the tissues of the sponge. Photosynthesis may suppress bioerosion and respiration may enhance bioerosion. A clear day/night inversion was seen in the pH-bioerosion response (Fig. 11a). The relative uptake of H^+ during photosynthesis in the thylakoid membranes of the symbiont chloroplasts could explain the negative correlation of pH with chemical bioerosion during the day (Table 6). An increase in (intracellular) [CO_2] due to respiration at night would theoretically increase [H^+] in conjunction with night bioerosion rates, but this was not observed in our experiment (Table 6, Fig. 11a). The unintended varying conditions of scenario 3 (Fig. 11a) revealed that night bioerosion rates were still higher than day rates despite a 51% decrease in [H^+] during night incubation. This may be an indication that the CO_2 released during night respiration by the sponge host and its associated symbionts is used in the underlying mechanisms of bioerosion. This would explain the positive correlation between pH and bioerosion at night (Table 6, Fig. 11a). Non-symbiotic species of *Cliona* may lack a differential response to day and night conditions if the cause is indeed due to symbiont photosynthesis or the higher overall night respiration seen in symbiont-bearing sponge species (Fang et al., 2014). Thus, repeating this experiment with a non-symbiotic bioeroding sponge could yield further insights into the effect of symbionts on the bioerosion process. Our observations suggest that [H^+] on its own accord does not seem to have a significant effect on chemical bioerosion rates. Instead, night bioerosion rates were enhanced even under increased pH conditions.

4.2.3 *The role of [HCO_3^-]*

As part of the natural covariance in the carbonate system, [HCO_3^-] varied considerably throughout the scenarios. Low [HCO_3^-] in combination with high [H^+] resulted in the highest bioerosion rates (scenario 4, Table 5). However, with our setup it is not possible to quantify the impact of [HCO_3^-] and understand if it is a forcing or simply a product of covariance. For example, [CO_3^{2-}] conditions were lowest in scenario 3 and resulted in high bioerosion rates, but this scenario also contained slightly lower [HCO_3^-] than in the other treatments. This may indicate that low [HCO_3^-] conditions may be favorable for bioerosion to occur, whereas high concentrations may impair bioerosion and enhance accretion by calcifying endolithic algae.

4.2.4 DIC dynamics

$DIC_{metabolism}$ and bioerosion rates correlated significantly (Table 6). $DIC_{metabolism}$ is expected to increase with respiration and decrease with photosynthesis. However, with no photosynthesis during the night, negative $DIC_{metabolism}$ values were still detected for a many incubated cores after night incubations (Table 4). Furthermore, despite ample sunlight during the day, some sponge cores still showed an increase in $DIC_{metabolism}$ (Fig. 11c). These unexpected responses may indicate an unknown bias in our DIC measurements. Control cores showed signs of photosynthesis during the day incubations, likely a result of endolithic algae that colonized these cores during acclimatization in the aquaria. Highest night bioerosion rates coincided with highest respiration rates (Fig. 11c). This may be explained by the fact that chemical bioerosion is a metabolically demanding process and without photosynthesis to offset this energetic cost, night bioerosion likely leads to higher respiration rates.

4.3 Mechanical bioerosion rates

Where chemical bioerosion rates vary amongst the applied incubation scenarios, the results for mechanical bioerosion do not vary consistently between treatments. Mechanical bioerosion was present in all incubations (Table 7, Fig. 12). Thus, mechanical and chemical bioerosion did occur in the treatments that showed net accretion, but were compensated by accretion rates. This implies that the accretion rates are slightly underestimated. The exceptionally high mechanical bioerosion rate in the night incubation of the scenario *N* is unlikely due to abnormally intense erosion and may result from an analytical error. The enhancement of chemical bioerosion in scenario 3 with respect to the control scenario is not reflected in the respective mechanical bioerosion data (Table 7, Fig. 12). Moreover, mechanical bioerosion rates were relatively constant among the conditions applied here. These observations suggests that sponge chip production rates are independent from chemical bioerosion rates.

4.4 Comparison of bioerosion rates

Comparing bioerosion rates (both chemical and mechanical) with published rates is only applicable for our control scenario since our manipulations have not yet been replicated. Wisshak et al. (2012) studied the bioerosion dynamics of *C. orientalis* and found combined (chem. + mech.) bioerosion rates of 2.23 ± 0.45 kg m^{-2} $year^{-1}$, about 4.5 times higher than our average combined rates for *C. caribbaea* (~0.51, Table 7). Rates found by Wisshak et al. (2012) are very similar to those found by Fang et al. (2013), who also reported 2.23 kg m^{-2} $year^{-1}$ for *C. orientalis*. A different study on *C. orientalis* by Wisshak et al. (2013) found chemical bioerosion rates of 0.09 ± 0.02, whereas our rates were ~4.3 times higher (0.39 ± 0.06, Table 5). The only apparent difference between the present-day conditions of these studies and our controls is the use of a different species of *Cliona*. Indeed, clionaids are known to vary substantially in their bioerosion capacity on a species level (Schönberg, 2008). Differences in nutrient conditions,

temperature, substrate structure and composition may all exert influence and could explain the discrepancies between published rates of *C. orientalis* and our results with *C. caribbaea*.

4.5 *Oxygen dynamics*

Possible (endolithic) algae colonization of the control cores is also supported by oxygen data. Day incubations of control cores resulted in higher than initial oxygen concentrations, indicating photosynthesis. This concurs with the observations of $DIC_{metabolism}$ decreases in these cores (Table 4). However, the oxygen content decrease associated with respiration during the night was only ~3%, suggesting that the total biomass of the algae was very limited. Sponge cores showed 2 to 4 times more variability in oxygen content during day and night incubations, and thus we can therefore assume that the control cores contained an insignificant biomass of photosynthetic organisms when compared to the sponge cores.

4.6 *Constraints of this study*

Interpretations of our results are bound by some constraints that should be considered. Firstly, physical contact with the cores was inevitable given the setup of the incubations and could damage or weaken the outer carbonate structure, making it more prone to break off during further handling and thus resulting in an overestimation of mechanical erosion rates . The accuracy of sponge chip sampling is further constrained by the possibility of sponge chips being produced and subsequently sticking to the sponge tissue/complex internal structure of *D. labyrinthiformis* and thus may have resulted in an underestimation of the mechanical bioerosion rates. These opposing biases on determined erosion rates hamper an accurate quantification of the absolute values for mechanical bioerosion rates and thereby the ratio between mechanical and chemical sponge bioerosion rates in our experiment.

The variability between sponge cores in terms of biomass, health and thus bioerosion potential induces uncertainty in the assessed rates, both chemical and mechanical. It is yet unknown if there is any experimental effect of sampling and acclimatizing sponges on cores and aquaria instead of natural conditions. Tissue that is damaged or exposed to fresh substrate may grow faster and bioerode more than the large sponge tissue patches found on dead corals, overestimating rates in experimental setups. This may introduce some degree of variability within and between treatments, but we assume this bias to be insignificant since natural variability in sponge colonies may be an equally important factor and can thus not be corrected for.

All batches were prepared and tested for initial values of DIC and T_A in the laboratory at CNSI, but the time interval between subsampling and start of the incubations varied between incubation rounds. Hence, the exact composition of the scenario may have varied slightly from the reported DIC and T_A. Because the changes in DIC and T_A were calculated in relation to this initial composition, any significant variability during this time interval would influence the

assessed chemical bioerosion rates. Since the batches were sealed and kept in the laboratory at constant temperature until use, we do not expect any significant effect on our study results.

The control cores experienced the same two week acclimatization period as the sponge cores, which probably allowed the colonization of (endolithic) algae on the cores, as oxygen analysis shows photosynthesis occurring on the control cores during the day and respiration during the night incubations (Fig. 11c). Rinsing of the control cores with fresh water prior to the experiments would have killed all marine life, yielding a better baseline for $DIC_{metabolism}$ data.

None of the carbonate parameters yielded significant correlations with control core chemical bioerosion rates, even though the coefficients were high (Table 6). This may be a cause of *n* needing to be larger for the control cores to discern an actual effect. Subsequent studies should employ more control cores for verification of these results. With none of the Ω values high enough to cause spontaneous aragonite precipitation (Fig. 11b), the presence of calcifying algae would explain the consistent pattern of accretion instead of bioerosion seen for the control cores (Table 5, Fig. 10).

$DIC_{metabolism}$ was calculated based on the change in T_A instead of independently assessed via in-situ oxygen data. Thus, any errors in the T_A data directly affect the outcome of $DIC_{metabolism}$, which in turn serves as an important measure of metabolic activity. However, the analytical error in the T_A measurements was only ± 1 µmol, making it highly unlikely that $DIC_{metabolism}$ values are affected.

The surface area of the cores was estimated from photographs with rulers adjacent to the cores for scale. Despite the complex structure of the *D. labyrinthiformis* and some degree of variability in topography per core, normalization of data for sponge tissue area yielded very similar results per treatment and thus we do not expect any bias in our data due to surface area measurement errors.

4.7 *The underlying mechanisms of sponge bioerosion*

The apparent dependence of bioerosion rates on $[CO_3^{2-}]$ and thereby Ω needs to be explained by a conceptual model for $CaCO_3$ dissolution by bioeroding sponges. Given our observations that: a) chemical bioerosion rates are consistently higher during the night, b) high $[H^+]$ alone did not constitute a forcing of bioerosion, c) Ω significantly influences bioerosion potential, and d) mechanical bioerosion remained constant despite changing water chemistry, we pose that the conditions at night (i.e. lack of photosynthesis) are important in enhancing the chemical bioerosion potential, possibly with a link to Ω.

The role of Ω in the dissolution process was already proposed by Hatch (1980): *'… the mechanism of excavation involves a localized modification of the calcium carbonate solubility equilibrium'*, p. 135-136. Looking specifically at sponges' etching cells and sites, Pomponi (1979, 1980) found that the activity of the carbonic anhydrase enzyme was associated with etching cell bodies and their activity. Another enzyme, acid phosphatase, seemed to be most active on the outer surfaces of the cell processes. This research suggested therefore that acid

phosphatase was involved in the extra- and intracellular digestion of organic components in the carbonate substrate, whereas carbonic anhydrase likely played a role in the dissolution of the carbonate itself. Hatch (1980) provided the first biochemical evidence of carbonic anhydrase being involved in determining Ω at the site of dissolution: a) since there is a positive correlation between the excavation activity of the sponge and the level of carbonic anhydrase in the sponge tissues, b) enzyme activity was concentrated in the cortical tissues of the bioeroding sponges, a region that is most likely to come in contact with fresh carbonate substrate, and c) inhibition of carbonic anhydrase significantly decreased bioerosion rates. Summarizing these observations, Hatch posed that the primary mechanism for the dissolution of calcium carbonate involves a shift in Ω within the microenvironment created the etching cell, mediated through the activity of carbonic anhydrase.

4.8 *Towards a model for sponge bioerosion*

4.8.1 *A role of carbonic anhydrase in bioerosion*

Of all the carbonate system parameters manipulated in our study, chemical bioerosion was most directly linked to Ω. In our experiment, this was conceived by manipulation of the general seawater chemistry, but a similar result may be achieved locally by the activity of carbonic anhydrase at the etching interface (Pomponi, 1979, 1980). Our results, together with the findings by Hatch and Pomponi, warrant further inquiry into the possible role of this enzyme in the bioerosion process.

The question remains how carbonic anhydrase, its substrates and products fit into the overall framework of chemical processes involved in sponge bioerosion. A conceptual model of sponge bioerosion could involve this enzyme as a driver for carbonate dissolution. Carbonic anhydrase is capable of very high substrate conversion rates and its rate is typically limited by the diffusion rate of its substrates (Lindskog, 1997). The reaction catalyzed by carbonic anhydrase is:

$$CO_2 + H_2O \leftrightarrow H_2CO_3 \leftrightarrow H^+ + HCO_3^- \qquad (9)$$

Equation 9 is reversible and runs from left to right when catalyzed by carbonic anhydrase II, and the reverse by carbonic anhydrase I. There is, at least superficially, a resemblance between the function of sponge etching cells and the osteoclasts responsible for resorption of bone material. Osteoclasts are common cells in the human body, responsible for breaking down old or damaged bone after an injury has occurred. The chemical composition of bone is different from calcium carbonate. Bone consists mainly of the mineral hydroxyapatite, an insoluble salt of calcium and phosphorus. Thus, bone dissolution by osteoclasts yields reaction products that differ from those produced by calcium carbonate dissolution. Despite this difference, the pattern of dissolution by osteoclasts bears some resemblances with the patterns produced by sponge chip production (Pomponi, 1980). However, osteoclasts do not produce chips but wholly resorb the bone mineral

(Arnett, 2013). The enzyme carbonic anhydrase is also present in osteoclasts and is known to play a major role in bone dissolution (Arnett, 2013). The question remains how carbonic anhydrase could contribute to the dissolution mechanisms in bioeroding sponges and how our results can be explained by these processes.

4.8.2 *Linking climate change with increased sponge bioerosion*

The significant increase in sponge bioerosion under elevated [CO_2] scenarios is well documented (Fang et al., 2013, 2014; Stubler et al., 2014, 2015; Wisshak et al., 2012, 2013). Given the presence of carbonic anhydrase II in sponge etching cells (Hatch, 1980; Pomponi, 1979, 1980; Schönberg, 2008), it is likely that this enzyme fulfills a role similar to that found in osteoclasts: the reaction of carbonic anhydrase II and CO_2 produces H^+ ions that, combined with Cl^-, form the hydrochloric acid necessary to dissolve carbonate. The speed of carbonate dissolution is thus dependent on [CO_2]. Given this dependence on [CO_2], the results of these previous workers could be explained via a hypothetical model for sponge bioerosion (Fig. 14).

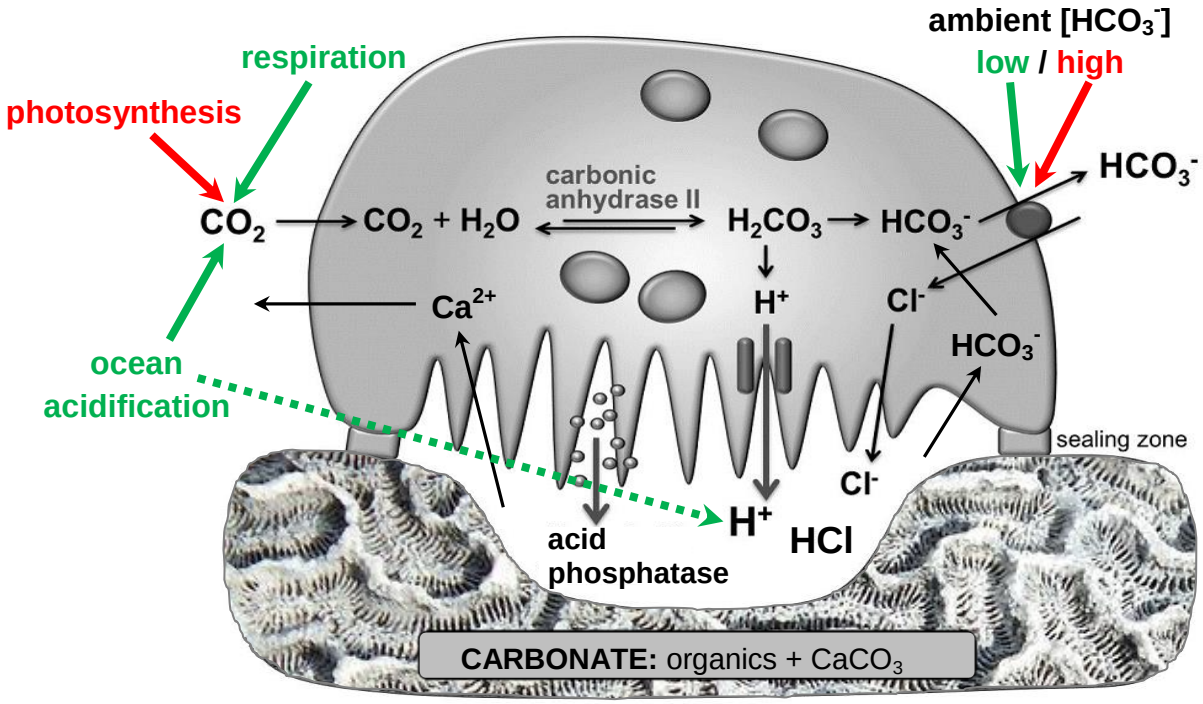

Fig. 14. A hypothetical model for sponge bioerosion by an etching cell. Carbonic anhydrase II catalyzes the formation of carbonic acid (H_2CO_3) which quickly dissociates. The resulting HCO_3^- is removed from the cell via a chloride-bicarbonate exchanger and H^+ and Cl^- are transported into a cavity covered by the etching cell. This cavity is sealed off from the surrounding medium by protein-bound sealing zones. The H^+ and Cl^- combine in the cavity to produce hydrochloric acid, significantly lowering Ω and inducing dissolution. However, the dissolution of carbonate yields reaction products Ca^{2+} and HCO_3^-. The continuous flushing of reaction these products from the cavity and interior of the cell maximizes the bioerosion potential. Acid phosphatase is secreted into the cavity to digest the organic components released during dissolution. Controls that enhance (green) or suppress (red) bioerosion rates are drawn. Figure modified from Arnett (2013).

A higher concentration of CO_2 under future climate scenarios would increase the potential for acid production and thus carbonate dissolution. Furthermore, a dependence on [CO_2] could explain our observations of consistently higher night bioerosion rates (Table 5); carbonic anhydrase II could be in competition with photosynthesis for CO_2 during the day, resulting in a suppressed bioerosion potential (Fig. 14). Conversely, at night photosynthesis cannot occur and respiration is increased, providing a readily available source of CO_2 for the bioerosion process. The presence of symbiotic algae of the *Symbodinium* family may thus partially suppress day bioerosion rates through photosynthesis. However, symbiont-bearing sponge species display significant gains in absolute rates of bioerosion, tissue penetration and growth with higher symbiont densities (Hill, 1996). The autotrophic carbon released by the symbionts contributes substantially towards the host sponge carbon budget (Fang et al., 2014). Therefore, the overall gain of having symbionts in a given sponge species is likely far greater than their effect on day bioerosion rates.

4.8.3 *Flushing as a limiting factor for bioerosion*

During chemical bioerosion, $CaCO_3$ is converted into Ca^{2+} and CO_3^{2-}, after which CO_3^{2-} reacts with free H^+ to form HCO_3^-. To increase bioerosion potential, the etching cell would need to maximize the amount of H^+ and Cl^- in the cavity, whilst continuously flushing out the reaction products Ca^{2+} and HCO_3^- to the surrounding water (Fig. 14). Pumping of H^+ into and Ca^{2+} out of the cavity in a 2:1 ratio would result in a stable charge balance. Likewise, the removal of HCO_3^- whilst adding Cl^- would also result in a balance. If HCO_3^- is not removed from the interior and cavity of the etching cell, continuing HCO_3^- production by carbonic anhydrase II and dissolution in the cavity would create an unfavorable [HCO_3^-] gradient, and dissolution ceases. This mechanism could explain the strong negative correlation in our study between [HCO_3^-] and bioerosion rates (Table 6).

The removal of HCO_3^- can only occur efficiently if [HCO_3^-] outside of the etching cell is relatively low. A high [HCO_3^-] in the surrounding medium could thus potentially limit bioerosion rates. Future studies which manipulate [HCO_3^-] independently of the other carbonate parameters could test this hypothesis. However, working with incubation chambers limits the flushing of Ca^{2+} and HCO_3^- since chamber water volume is limited and exchange with external water cannot occur. Increased night bioerosion rates, as seen in our study, would require more flushing of HCO_3^- from the etching cells and ultimately, the sponge. An increase in ambient [HCO_3^-] in the incubation chamber due to this process would increase the pH, explaining the positive correlation between pH and [HCO_3^-] during our night incubations (Table 6, Fig. 11a). Under natural conditions, clionaid sponges would clearly not experience this limitation. Thus, the question arises whether the incubation method limits these physiological processes.

The volume of the water enclosed by the etching cell plays an important role in the dissolution process; a relatively small volume would aid rapid acidification and the subsequent lowering of Ω to induce dissolution. However, upon dissolution of the carbonate substrate, Ω

would increase more rapidly in a relatively small volume than in a larger volume of water. This increase in Ω would hamper further dissolution from occurring. To achieve a maximum bioerosion potential, the etching cell must thus keep the volume for acidification relatively small whilst mitigating the subsequent increase in Ω when dissolution occurs. Continuous cycles of acidification, dissolution and flushing of the water volume with ambient, relatively lower Ω water would keep the bioerosion potential high. The speed of these cycles may thus be limited by flushing rates. Flushing could occur by temporary opening of the sealing zones (Fig. 14) or even a total replacement of the etching cell. The latter may pose a mechanism to overcome unfavorable HCO_3^- gradients across the outer cell membrane by storing and exporting HCO_3^- inside discarded etching cells. Sponges are capable of rapid cell turnover (de Goeij et al., 2013) and this ability may play a yet undiscovered role in bioeroding sponges. Studies into the turnover of etching cells may reveal how flushing is achieved. The local addition of mitotic inhibitors may severely decrease bioerosion activity, proving a link between turnover rates and bioerosion potential.

In combination with flushing, the bioerosion process could be greatly aided by altering the carbonate species in the etching cell cavity. The conversion of HCO_3^- to CO_2 would mitigate the complex and potentially costly transport of HCO_3^- across the cell membranes (Fig. 14). Instead, CO_2 would be able to readily diffuse through the cell membranes, allowing carbonate dissolution to continue for longer without requiring flushing. This CO_2 may subsequently be used by either symbionts or carbonic anhydrase II (Fig. 14). However, significant proton pumping would be required to achieve pH < 6.5 upon dissolution of carbonate to immediately convert HCO_3^- to CO_2. Achieving a balanced model would require in-situ observations to confirm which processes are occurring, from which their relative contributions to bioerosion potential can be assessed.

4.8.4 *Ocean acidification reduces the metabolic cost of bioerosion*

In this experiment, bioerosion rates were most clearly related with $[CO_3^{2-}]$ and thereby, Ω. This suggests that a lower Ω in the surrounding water of the sponge is instrumental in enhancing bioerosion rates. With Ω already relatively low, the sponge expends less energy to acidify the etching cell cavity water mass for carbonate dissolution. Via this pathway, ocean acidification not only increases $[CO_2]$ as a possible substrate for internal processes, but may also decrease the energy costs of the dissolution process, enhancing bioerosion rates (Fig. 14, dotted arrow).

Solely a high $[H^+]$ did not yield bioerosion rates, whereas the combination of a low $[CO_3^{2-}]$ and high $[H^+]$ was more effective than low $[CO_3^{2-}]$ alone (Table 5). The main effect of high $[H^+]$ under ocean acidification is to decrease $[CO_3^{2-}]$ and Ω. High $[H^+]$ in itself does not induce enhanced bioerosion rates in clionaid sponges. The state of Ω seems to be the defining factor that governs whether and at which rate bioerosion occurs. These observations verify the link between $[H^+]$ and $[CO_3^{2-}]$ proposed by Fang et al. (2013) and Wisshak et al. (2012). A high $[H^+]$ in seawater could potentially amplify the H^+ gradient already created by the etching cell and thus reduce metabolic costs. Since symbiotic bioeroding sponges have a significant source of

additional energy through the process of photosynthesis (Fang et al., 2014), processes that decrease the energy costs of bioerosion cause an even greater surplus of energy available for bioerosion. Hence, non-symbiotic species may not be able to benefit from ocean acidification to the same extent as those that harbor symbionts.

Rising global temperatures due to climate change may also impact the metabolism of bioeroding sponges. The effect of rising sea surface temperatures could cause a parabolic response; increasing bioerosion rates up to a certain thermal threshold followed by a decline due to the sponges experiencing an overall negative energy balance as a result of metabolic costs (Fang et al., 2014). Such parabolic temperature responses have been reported by Wisshak et al. (2013) and Enochs et al. (2015) and may also be linked to disease and/or bleaching in symbiont-bearing clionaid sponges (Schönberg & Ortiz, 2008).

The key to unraveling why ocean acidification causes enhanced bioerosion rates may merely be due to an increased metabolic efficiency in the sponge organism by virtue of changing ocean chemistry. Whereas ongoing decreases in pH, Ω and available [CO_3^{2-}] are detrimental for calcifying organisms such as corals, these conditions provide an increasingly favorable setting for bioerosion to occur (Enochs et al., 2015; Wisshak et al., 2012). The molecular pathways suggested in our model concur with our results, but need to be verified by in-situ observations.

5. Conclusions

5.1 *Conclusions of this study*

By reducing the metabolic cost of both carbonate dissolution and the maintenance of ion gradients, the changes in chemistry due to ocean acidification enhance the bioerosion potential of clionaid sponges. Our hypothetical model for sponge bioerosion creates a framework in which our results can be placed and future study directions explored. Varying carbonate system parameters revealed that high [H^+] alone does not induce enhanced bioerosion. Instead, Ω constitutes a crucial threshold for bioeroding sponges; values above Ω ~ 4 result in the sponge being unable to reduce Ω enough for dissolution to occur. Thus, Ω is the defining factor that governs whether and at which rate bioerosion occurs. The process of flushing is a potentially limiting factor for bioerosion rates and requires detailed, in-situ observations to reveal its underlying mechanisms. With enhanced bioerosion in future oceans alongside a decreased reef building potential of corals and calcifying algae, it seems inevitable that carbonate budgets will become increasingly negative.

***5.2** Knowledge gaps and future research directions*

The phenomenon of enhanced sponge bioerosion rates under future climate scenarios has been extensively researched and confirmed. However, the molecular mechanisms involved in this process have not yet been researched in detail. Our model portrayed several possible pathways and mechanisms, but for now relies on theory only. Experimental observations are needed to verify these processes in-situ. A study complementary to ours could investigate the potential suppressing role of [HCO_3^-] in the bioerosion process by manipulation of this parameter in incubation experiments whilst keeping the other parameters fixed. The proposed competition of carbonic anhydrase II and photosynthesis for CO_2 would explain the difference between day and night incubation rates and warrants further investigation. Experiments on man-made, ^{13}C tagged calcite would allow tracking of the HCO_3^- ion after its production, possibly allowing for dissolution and flushing rate estimations in-situ. Comparison of symbiotic and non-symbiotic clionaid species may elucidate the internal forcings and homeostasis of the sponge organism during the bioerosion process. The reduction of metabolic costs for bioerosion by climate change represents an attractive hypothesis but requires controlled experiments focused on elucidating the patterns of energy expenditure under varying environmental conditions. Research into the interactions of live corals with clionaid sponges could shed light on their resilience to overgrowth and possible shifts in reef ecology associated with clionaid species expansion. Overall, more insight is needed into the molecular and ecological factors that make clionaids such successful constituents on coral reefs.

6. Acknowledgements

First of all, I would like to thank Alice Webb and Didier de Bakker for their persistence during the fieldwork on St. Eustatius for this study. It was a challenging project but also a very informative one for myself, learning new lab and field techniques as well as having the opportunity to join a research cruise, partake in extensive diving and mastering the art of troubleshooting. Dr. Steven van Heuven was instrumental in the success of our setup and has provided me with great guidance and feedback from which I have learned a lot. I would also like to thank Dr. Lennart de Nooijer and Prof. Dr. Gert-Jan Reichart for their guidance and for granting me the opportunity to participate in an internship at the NIOZ. Lastly, I want to thank my family and loved ones for all their support during my fieldwork and at home.

Mom, this one's for you

7. References

Acker, K. L., & Risk, M. J. (1985). Substrate destruction and sediment production by the boring sponge Cliona caribbaea on Grand Cayman Island. *Journal of Sedimentary Research*, *55*(5).

Alvarez-Filip, L., Dulvy, N. K., Gill, J. A., Côté, I. M., & Watkinson, A. R. (2009). Flattening of Caribbean coral reefs: region-wide declines in architectural complexity. *Proceedings of the Royal Society of London B: Biological Sciences*, *276*(1669), 3019-3025.

Anthony, K. R., Kline, D. I., Diaz-Pulido, G., Dove, S., & Hoegh-Guldberg, O. (2008). Ocean acidification causes bleaching and productivity loss in coral reef builders. *Proceedings of the National Academy of Sciences*,*105*(45), 17442-17446.

Anthony, K., Maynard, J. A., Diaz-Pulido, G., Mumby, P. J., Marshall, P. A., Cao, L., & Hoegh-Guldberg, O. (2011). Ocean acidification and warming will lower coral reef resilience. *Global Change Biology*, *17*(5), 1798-1808.

Arnett, T. R. (2013). Osteoclast biology. *Osteoporosis. Elsevier, Oxford*, 149-160.

Aronson, R. B., & Precht, W. F. (2001). White-band disease and the changing face of Caribbean coral reefs. In *The ecology and etiology of newly emerging marine diseases* (pp. 25-38). Springer Netherlands.

Bellwood, D. R., Hughes, T. P., Folke, C., & Nyström, M. (2004). Confronting the coral reef crisis. *Nature*, *429*(6994), 827-833.

Bourne, D., Iida, Y., Uthicke, S., & Smith-Keune, C. (2008). Changes in coral-associated microbial communities during a bleaching event. *The ISME journal*, *2*(4), 350-363.

Burge, C. A., Eakin, C. M., Friedman, C. S., Froelich, B., Hershberger, P. K., Hofmann, E. E., ... & Ford, S. E. (2014). Climate change influences on marine infectious diseases: implications for management and society. *Marine Science*, *6*.

Canadell, J. G., Le Quéré, C., Raupach, M. R., Field, C. B., Buitenhuis, E. T., Ciais, P., ... & Marland, G. (2007). Contributions to accelerating atmospheric CO2 growth from economic activity, carbon intensity, and efficiency of natural sinks. *Proceedings of the national academy of sciences*, *104*(47), 18866-18870.

Carballo, J. L., Bautista, E., Nava, H., Cruz-Barraza, J. A., & Chávez, J. A. (2013). Boring sponges, an increasing threat for coral reefs affected by bleaching events. *Ecology and evolution*, *3*(4), 872-886.

co2.earth. Retrieved March 9, 2016, from https://www.co2.earth/

de Goeij, J. M., van Oevelen, D., Vermeij, M. J., Osinga, R., Middelburg, J. J., de Goeij, A. F., & Admiraal, W. (2013). Surviving in a marine desert: the sponge loop retains resources within coral reefs. *Science*, *342*(6154), 108-110.

DeCarlo, T. M., Cohen, A. L., Barkley, H. C., Cobban, Q., Young, C., Shamberger, K. E., ... & Golbuu, Y. (2015). Coral macrobioerosion is accelerated by ocean acidification and nutrients. *Geology*, *43*(1), 7-10.

Dickson, A. G., Sabine, C. L., & Christian, J. R. (2007). Guide to Best Practices for Ocean CO2 Measurements.

Dufault, A. M., Cumbo, V. R., Fan, T. Y., & Edmunds, P. J. (2012). Effects of diurnally oscillating pCO2 on the calcification and survival of coral recruits. *Proceedings of the Royal Society of London B: Biological Sciences*, rspb20112545.

Eakin, C. M., Morgan, J. A., Heron, S. F., Smith, T. B., Liu, G., Alvarez-Filip, L., ... & Brandt, M. (2010). Caribbean corals in crisis: record thermal stress, bleaching, and mortality in 2005. *PloS one*, *5*(11), e13969.

Endean, R. (1976). Destruction and recovery of coral reef communities. *Biology and Geology of Coral Reefs. Vol. 3, Biology*, *2*, 215-254.

Enochs, I. C., Manzello, D. P., Carlton, R. D., Graham, D. M., Ruzicka, R., & Colella, M. A. (2015). Ocean acidification enhances the bioerosion of a common coral reef sponge: implications for the persistence of the Florida

Reef Tract. *Bulletin of Marine Science*, *91*(2), 271-290.

Fang, J. K., Mello-Athayde, M. A., Schönberg, C. H., Kline, D. I., Hoegh-Guldberg, O., & Dove, S. (2013). Sponge biomass and bioerosion rates increase under ocean warming and acidification. *Global change biology*,*19*(12), 3581-3591.

Fang, J. K., Schönberg, C. H., Mello-Athayde, M. A., Hoegh-Guldberg, O., & Dove, S. (2014). Effects of ocean warming and acidification on the energy budget of an excavating sponge. *Global change biology*, *20*(4), 1043-1054.

Gardner, T. A., Côté, I. M., Gill, J. A., Grant, A., & Watkinson, A. R. (2003). Long-term region-wide declines in Caribbean corals. *Science*, *301*(5635), 958-960.

Glynn, P. W. (1988). El Nino warming, coral mortality and reef framework destruction by echinoid bioerosion in the eastern Pacific. *Galaxea*, *7*, 129-160.

Glynn, P. W., & Manzello, D. P. (2015). Bioerosion and coral reef growth: a dynamic balance. In *Coral Reefs in the Anthropocene* (pp. 67-97). Springer Netherlands.

Hatch, W. I. (1980). The implication of carbonic anhydrase in the physiological mechanism of penetration of carbonate substrata by the marine burrowing sponge Cliona celata (Demospongiae). *The Biological Bulletin*, *159*(1), 135-147.

Hill, M. S. (1996). Symbiotic zooxanthellae enhance boring and growth rates of the tropical sponge Anthosigmella varians forma varians. *Marine Biology*, *125*(4), 649-654.

Hoegh-Guldberg, O., Mumby, P. J., Hooten, A. J., Steneck, R. S., Greenfield, P., Gomez, E., ... & Knowlton, N. (2007). Coral reefs under rapid climate change and ocean acidification. *science*, *318*(5857), 1737-1742.

Holmes, K. E. (2000). Effects of eutrophication on bioeroding sponge communities with the description of new West Indian sponges, Cliona spp.(Porifera: Hadromerida: Clionidae). *Invertebrate Biology*, *119*(2), 125-138.

Hönisch, B., Ridgwell, A., Schmidt, D. N., Thomas, E., Gibbs, S. J., Sluijs, A., ... & Kiessling, W. (2012). The geological record of ocean acidification. S*cience*, *335*(6072), 1058-1063.

Hughes, T. P. (1994). Catastrophes, phase shifts, and large-scale degradation of a Caribbean coral reef. *Science-AAAS-Weekly Paper Edition*,*265*(5178), 1547-1551.

Hughes, T. P., Baird, A. H., Bellwood, D. R., Card, M., Connolly, S. R., Folke, C., ... & Lough, J. M. (2003). Climate change, human impacts, and the resilience of coral reefs. *science*, *301*(5635), 929-933.

Jackson, J. B., Kirby, M. X., Berger, W. H., Bjorndal, K. A., Botsford, L. W., Bourque, B. J., ... & Hughes, T. P. (2001). Historical overfishing and the recent collapse of coastal ecosystems. *science*, *293*(5530), 629-637.

Kennedy, E. V., Perry, C. T., Halloran, P. R., Iglesias-Prieto, R., Schönberg, C. H., Wisshak, M., ... & Mumby, P. J. (2013). Avoiding coral reef functional collapse requires local and global action. *Current Biology*, *23*(10), 912-918.

Kleypas, J. A., McManus, J. W., & Meñez, L. A. (1999). Environmental limits to coral reef development: where do we draw the line?. *American Zoologist*, *39*(1), 146-159.

Kleypas, J. A., & Langdon, C. (2006). Coral reefs and changing seawater carbonate chemistry. *Coral reefs and climate change: science and management*, 73-110.

Langdon, C., & Atkinson, M. J. (2005). Effect of elevated pCO2 on photosynthesis and calcification of corals and interactions with seasonal change in temperature/irradiance and nutrient enrichment. *Journal of Geophysical Research: Oceans*, *110*(C9).

Lindskog, S. (1997). Structure and mechanism of carbonic anhydrase. *Pharmacology & therapeutics*, *74*(1), 1-20.

López-Victoria, M., & Zea, S. (2004). Storm-mediated coral colonization by an excavating Caribbean sponge. *Climate Research.*, *26*(3), 251-256.

Lüthi, D., Le Floch, M., Bereiter, B., Blunier, T., Barnola, J. M., Siegenthaler, U., ... & Stocker, T. F. (2008). High-resolution carbon dioxide

concentration record 650,000–800,000 years before present. *Nature*, *453*(7193), 379-382.

Márquez, J. C., Zea, S., & López-Victoria, M. (2006). Is competition for space between the encrusting excavating sponge Cliona tenuis and corals influenced by higher-than-normal temperatures?. *Boletín de Investigaciones Marinas y Costeras-Invemar*, *35*(1), 259-265.

Marubini, F., Ferrier-Pagès, C., Furla, P., & Allemand, D. (2008). Coral calcification responds to seawater acidification: a working hypothesis towards a physiological mechanism. *Coral Reefs*, *27*(3), 491-499.

McCulloch, M., Fallon, S., Wyndham, T., Hendy, E., Lough, J., & Barnes, D. (2003). Coral record of increased sediment flux to the inner Great Barrier Reef since European settlement. *Nature*, *421*(6924), 727-730.

McCulloch, M., Falter, J., Trotter, J., & Montagna, P. (2012). Coral resilience to ocean acidification and global warming through pH up-regulation. *Nature Climate Change*, *2*(8), 623-627.

Mintrop, L., Pérez, F. F., González-Dávila, M., Santana-Casiano, M., & Körtzinger, A. (2000). Alkalinity determination by potentiometry: Intercalibration using three different methods.

Moberg, F., & Folke, C. (1999). Ecological goods and services of coral reef ecosystems. *Ecological economics*, *29*(2), 215-233.

Montaggioni, L. F., & Braithwaite, C. J. (2009). *Quaternary coral reef systems: history, development processes and controlling factors* (Vol. 5). Elsevier.

Nakamura, M., Ohki, S., Suzuki, A., & Sakai, K. (2011). Coral larvae under ocean acidification: survival, metabolism, and metamorphosis. *PLoS One*,*6*(1), e14521.

Nava, H., & Carballo, J. L. (2008). Chemical and mechanical bioerosion of boring sponges from Mexican Pacific coral reefs. *Journal of experimental Biology*, *211*(17), 2827-2831.

Neumann, A. C. (1966). Observations on coastal erosion in Bermuda and measurements of the boring rate of the sponge, Cliona lampa. *Limnology and Oceanography*, *11*(1), 92-108.

Pandolfi, J. M., Bradbury, R. H., Sala, E., Hughes, T. P., Bjorndal, K. A., Cooke, R. G., ... & Warner, R. R. (2003). Global trajectories of the long-term decline of coral reef ecosystems. *Science*, *301*(5635), 955-958.

Pandolfi, J. M., Connolly, S. R., Marshall, D. J., & Cohen, A. L. (2011). Projecting coral reef futures under global warming and ocean acidification.*science*, *333*(6041), 418-422.

Payri, C. E. (1997). Hydrolithon reinboldii rhodolith distribution, growth and carbon production of a French Polynesian reef. In *Proceedings of the 8th international coral reef symposium* (Vol. 1, pp. 755-760).

Perry, C. T., Edinger, E. N., Kench, P. S., Murphy, G. N., Smithers, S. G., Steneck, R. S., & Mumby, P. J. (2012). Estimating rates of biologically driven coral reef framework production and erosion: a new census-based carbonate budget methodology and applications to the reefs of Bonaire. *Coral Reefs*, *31*(3), 853-868.

Perry, C. T., Murphy, G. N., Kench, P. S., Edinger, E. N., Smithers, S. G., Steneck, R. S., & Mumby, P. J. (2014). Changing dynamics of Caribbean reef carbonate budgets: emergence of reef bioeroders as critical controls on present and future reef growth potential. *Proceedings of the Royal Society of London B: Biological Sciences*, *281*(1796), 20142018.

Perry, C. T., Murphy, G. N., Kench, P. S., Smithers, S. G., Edinger, E. N., Steneck, R. S., & Mumby, P. J. (2013). Caribbean-wide decline in carbonate production threatens coral reef growth. *Nature communications*, *4*, 1402.

Perry, C. T., Spencer, T., & Kench, P. S. (2008). Carbonate budgets and reef production states: a geomorphic perspective on the ecological phase-shift concept. *Coral Reefs*, *27*(4), 853-866.

Petit, J. R., Jouzel, J., Raynaud, D., Barkov, N. I., Barnola, J. M., Basile, I., ... & Delmotte, M. (1999). Climate and atmospheric history of the past 420,000 years from the Vostok ice core, Antarctica. *Nature*, *399*(6735), 429-436.

Lewis, E., Wallace, D., & Allison, L. J. (1998). *Program developed for CO2 system calculations* (p. 38). Tennessee: Carbon Dioxide Information Analysis Center, managed by Lockheed Martin Energy Research Corporation for the US Department of Energy.

Pomponi, S. A. (1979). Ultrastructure and cytochemistry of the etching area of boring sponges. *Coll. Int. CNRS*, *291*, 317-332.

Pomponi, S. A. (1980). Cytological mechanisms of calcium carbonate excavation by boring sponges. *Int Rev Cytol*, *65*, 301-319.

Raven, J., Caldeira, K., Elderfield, H., Hoegh-Guldberg, O., Liss, P., Riebesell, U., ... & Watson, A. (2005). *Ocean acidification due to increasing atmospheric carbon dioxide*. The Royal Society.

Rose, C. S., & Risk, M. J. (1985). Increase in Cliona delitrix infestation of Montastrea cavernosa heads on an organically polluted portion of the Grand Cayman fringing reef. *Marine Ecology*, *6*(4), 345-363.

Rützler, K. (2002). Impact of crustose clionid sponges on Caribbean reef corals. *Acta Geologica Hispanica*, *37*(1), 61-72.

Rützler, K., & Rieger, G. (1973). Sponge burrowing: fine structure of Cliona lampa penetrating calcareous substrata. *Marine Biology*, *21*(2), 144-162.

Sabine, C. L., Feely, R. A., Gruber, N., Key, R. M., Lee, K., Bullister, J. L., ... & Millero, F. J. (2004). The oceanic sink for anthropogenic CO2. *science*,*305*(5682), 367-371.

Schönberg, C. H. L., & Ortiz, J. C. (2008, July). Is sponge bioerosion increasing. In *Proceedings of 11th Int Coral Reef Symp* (pp. 7-11).

Schönberg, C. H. (2008). A history of sponge erosion: from past myths and hypotheses to recent approaches. In *Current Developments in Bioerosion*(pp. 165-202). Springer Berlin Heidelberg.

Schönberg, C. H., & Suwa, R. (2007). Why bioeroding sponges may be better hosts for symbiotic dinoflagellates than many corals. *Porifera Research: Biodiversity, Innovation and Sustainability. Publ Museu Nac Rio de Janeiro*, 569-580.

Schönberg, C. H., Suwa, R., Hidaka, M., & Loh, W. K. W. (2008). Sponge and coral zooxanthellae in heat and light: preliminary results of photochemical efficiency monitored with pulse amplitude modulated fluorometry. *Marine Ecology*, *29*(2), 247-258.

Stearn, C. W., Scoffin, T. P., & Martindale, W. (1977). Calcium Carbonate Budget of a Fringing Reef on the West Coast of BarbadosPart I—Zonation and Productivity. *Bulletin of Marine Science*, *27*(3), 479-510.

Solomon, S. (Ed.). (2007). *Climate change 2007-the physical science basis: Working group I contribution to the fourth assessment report of the IPCC*(Vol. 4). Cambridge University Press.

Stubler, A. D., Furman, B. T., & Peterson, B. J. (2014). Effects of pCO2 on the interaction between an excavating sponge, Cliona varians, and a hermatypic coral, Porites furcata. *Marine biology*, *161*(8), 1851-1859.

Stubler, A. D., Furman, B. T., & Peterson, B. J. (2015). Sponge erosion under acidification and warming scenarios: differential impacts on living and dead coral. *Global change biology*, *21*(11), 4006-4020.

Stumm, W., & Morgan, J. J. (1981). *Aquatic chemistry: an introduction emphasizing chemical equilibria in natural waters*. John Wiley.

Tribollet, A., Godinot, C., Atkinson, M., & Langdon, C. (2009). Effects of elevated pCO2 on dissolution of coral carbonates by microbial euendoliths. *Global Biogeochemical Cycles*, *23*(3).

Vecsei, A. (2004). A new estimate of global reefal carbonate production including the fore-reefs. *Global and Planetary Change*, *43*(1), 1-18.

Veron, J. E. (2011). Ocean acidification and coral reefs: an emerging big picture. *Diversity*, *3*(2), 262-274.

Veron, J. E. N., Hoegh-Guldberg, O., Lenton, T. M., Lough, J. M., Obura, D. O., Pearce-Kelly, P., ... & Rogers, A. D. (2009). The coral reef crisis: The critical importance of< 350ppm CO 2. *Marine Pollution Bulletin*, *58*(10), 1428-1436.

Williams, D. M., Roth, C. H., Reichelt, R., Ridd, P., Rayment, G. E., Larcombe, P., ... & Furnas, M. (2002). The current level of scientific understanding on impacts of terrestrial run-off on the Great Barrier Reef World Heritage Area. *CRC Reef Research Centre, Townsville, Australia*.

Wisshak, M., Schönberg, C. H., Form, A., & Freiwald, A. (2012). Ocean acidification accelerates reef bioerosion. *PLoS One*, *7*(9), e45124.

Wisshak, M., Schönberg, C. H., Form, A. U., & Freiwald, A. (2013). Effects of ocean acidification and global warming on reef bioerosion—lessons from a clionaid sponge. *Aquatic Biology*, *19*(2), 111-127.

Wolf-Gladrow, D. A., Zeebe, R. E., Klaas, C., Körtzinger, A., & Dickson, A. G. (2007). Total alkalinity: The explicit conservative expression and its application to biogeochemical processes. *Marine Chemistry*, *106*(1), 287-300.

Zundelevich, A., Lazar, B., & Ilan, M. (2007). Chemical versus mechanical bioerosion of coral reefs by boring sponges-lessons from Pione cf. vastifica. *Journal of experimental biology*, *210*(1), 91-96.